

Bridging the Gap between Spatial and Spectral Domains: A Theoretical Framework for Graph Neural Networks

ZHIQIAN CHEN, Department of Computer Science and Engineering, Mississippi State University, U.S.A
FANGLAN CHEN, Department of Computer Science, Virginia Tech, U.S.A
LEI ZHANG, Department of Computer Science, Virginia Tech, U.S.A
TAORAN JI, Department of Computer Science, Virginia Tech, U.S.A
KAIQUN FU, Department of Computer Science, Virginia Tech, U.S.A
LIANG ZHAO, Department of Computer Science, Emory University, U.S.A
FENG CHEN, Department of Computer Science, The University of Texas at Dallas, U.S.A
LINGFEI WU, JD.COM Silicon Valley Research Center, U.S.A
CHARU AGGARWAL, IBM T. J. Watson Research Center, U.S.A
CHANG-TIEN LU, Department of Computer Science, Virginia Tech, U.S.A

During the past decade, deep learning’s performance has been widely recognized in a variety of machine learning tasks, ranging from image classification, speech recognition to natural language understanding. Graph neural networks (GNN) are a type of deep learning that is designed to handle non-Euclidean issues using graph-structured data that are difficult to solve with traditional deep learning techniques. The majority of GNNs were created using a variety of processes, including random walk, PageRank, graph convolution, and heat diffusion, making direct comparisons impossible. Previous studies have primarily focused on classifying current models into distinct categories, with little investigation of their internal relationships. This research proposes a unified theoretical framework and a novel perspective that can methodologically integrate existing GNN into our framework. We survey and categorize existing GNN models into spatial and spectral domains, as well as show linkages between subcategories within each domain. Further investigation reveals a strong relationship between the spatial, spectral, and subgroups of these domains.

1 INTRODUCTION

Deep learning’s performance in various machine learning tasks [52, 66, 85, 105, 107, 123] has been extensively recognized in recent decades, with amazing success on Euclidean data. In recent decades, a slew of new applications have emerged in which effective information analysis boils down to the non-Euclidean geometry of data represented by a graph, such as social networks [65], transportation networks [9], spread of epidemic disease [93], brain’s neuronal networks [86], gene data on biological regulatory networks [32], telecommunication networks [36], and knowledge graph [77] and so on. Previous deep learning algorithms, such as convolutional neural networks and recurrent neural networks, couldn’t handle such non-Euclidean problems on graph-structured data. Modeling data using a graph is difficult because graph data is irregular, i.e., each graph has a different number of nodes and each node in a graph has a varied number of neighbors, making some operations like convolutions inapplicable to the network structure.

There has recently been a surge growing interest in applying deep learning to graph data. Inspired by deep learning’s success, principles from deep learning models are used to handle the graph’s

Authors’ addresses: Zhiqian Chen, zchen@cse.msstate.edu, Department of Computer Science and Engineering, Mississippi State University, U.S.A; Fanglan Chen, fanglanc@vt.edu, Department of Computer Science, Virginia Tech, U.S.A; Lei Zhang, zhanglei@vt.edu, Department of Computer Science, Virginia Tech, U.S.A; Taoran Ji, jtr@vt.edu, Department of Computer Science, Virginia Tech, U.S.A; Kaiqun Fu, fukaiqun@vt.edu, Department of Computer Science, Virginia Tech, U.S.A; Liang Zhao, liang.zhao@emory.edu, Department of Computer Science, Emory University, Falls Church, U.S.A; Feng Chen, feng.chen@utdallas.edu, Department of Computer Science, The University of Texas at Dallas, U.S.A; Lingfei Wu, lingfei.wu@jd.com, JD.COM Silicon Valley Research Center, U.S.A; Charu Aggarwal, charu@us.ibm.com, IBM T. J. Watson Research Center, U.S.A; Chang-Tien Lu, Department of Computer Science, Virginia Tech, U.S.A, ctlu@vt.edu.

inherent complexity. This growing trend has piqued the interest of the machine learning community, and a huge number of GNN models have been constructed based on diverse theories [7, 21, 35, 47, 61, 115] and grouped into coarse-grained groupings like the spectral [48, 92, 124, 139, 142] and spatial [7, 47, 115] domains. Despite the fact that GNNs have dominated graph representation learning in recent years, their representational effectiveness and physical meaning are still poorly understood. The lack of a consistent framework for GNN makes comparing and improving state-of-the-art approaches extremely difficult. Because black box models may be associated with unmanageable hazards, this limitation makes it tough to employ GNN in many high-stakes fields such as business intelligence or drug research. As a result, there is a compelling need to demystify GNN, prompting academics to look for a more generalized framework. The main problem is that existing GNN models use a variety of techniques, including random walks, Page Rank, attention models, low-pass filters, message forwarding, and so on. Some preliminary research can only explain a few GNN methods [44, 127, 132], leaving the majority of GNN methods unaccounted for. Previous GNN surveys [48, 92, 124, 139, 142] have focused on dividing numerous current models into discrete groups and elaborating on each group without considering their relationship.

This research tries to give a cohesive framework for generalizing GNN, bridging the gap between seemingly independent works in the spatial and spectral domains. This research focuses on the connections between GNN from a unified theoretical approach, moving beyond existing taxonomies and building a new GNN paradigm. Our research is unusual in that it connects diverse GNNs, allowing all GNN models to be rethought. It should be noted that the majority of the work presented is related to Graph Convolution Networks (GCN) [61], which is the most common type of GNN, and that many other varieties of GNN are still based on GCN. As a result, we do not differentiate between GNN and GCN in this context and refer to GNN in the following sections.

1.1 Graph Neural Networks in Spatial and Spectral Domain

GNN versions have recently received a lot of attention. However, the existence of numerous GNNs complicates model selection because they are not easily understood. First, spectral theory is used to create certain early techniques [35, 49], while spatial theory is used to propose others [47]. It is impossible to compare spectral and spatial techniques due to their intrinsic mismatch. Second, even within each area, models differ greatly, making it difficult to evaluate their benefits and drawbacks.

To untangle the mess, we present a comprehensive framework that connects the spatial and spectral domains and reveals their intricate relationship. Furthermore, both domains' subcategories are proven to have a hierarchical link. Many well-known GNN will be used to demonstrate the universality of our architecture. The focus on a unified framework adds to the knowledge of how GNN operates. The goal of this research is to use a combination of spectral graph theory and approximation theory to investigate the relationship between important categories, such as spatial and spectral-based approaches. We give a detailed analysis of GNN's current research findings in this paper, as well as a discussion of specific jobs that require future examination. This article's main motivation is twofold:

- (1) **Connecting the spectral and spatial domains.** The fundamental concepts, principles, and physical implications of spectral- and spatial-based GNN are significantly different due to their distinct features. As a result, we present an overview of the fundamental principles and properties of spectral- and spatial-based GNN in order to help people better grasp the problems, potential, and necessity of GNN. Formally, a rigorous equivalence is discovered, demonstrating that function on connectedness is equivalent to eigenspace filtering.
- (2) **Dissecting spectral and spatial domains, respectively.** Filtering functions on eigenvalues are investigated in spectral approaches, and the filtering function choice can be aligned with

different strategies in approximation theory. While attributes aggregation, which can be understood from the size and direction within a predetermined region, is investigated with spatial approaches.

The following is a summary of the article’s structure: In Section 2, we cover techniques to representing the graph, spectral-based GNNs, spatial-based GNNs, and necessary fundamentals, as well as basic concepts, unique principles, and attributes of graph neural networks. Section 3 provides an overview of the proposed framework and emphasizes the hierarchy’s importance. Under our suggested taxonomy framework, we revisit representative GNN models in each domain from Section 4 to Section 5. In Section 6, we thoroughly examine the benefits and drawbacks of each domain, providing practical advice on GNN model selection. Section 7 also provides a case study with our approaches, demonstrating our suggested framework with relevant and trending issues in GNN. The survey’s readers should have a fundamental understanding of graphs, such as adjacency matrices and graph Laplacian, as well as graph signal processing techniques, eigen-decomposition, deep learning techniques.

1.2 Related Surveys and Our Contributions

Recently, a number of extensive surveys on graph neural networks have been compiled [20, 48, 124, 139, 142, 145]. Instead of studying their hierarchical and underlying mechanisms, most existing surveys focus on gathering newly published works and categorizing them into separate categories. A detailed survey, in particular, provides an overview of many examples of graph neural networks, classifying them as spatial or spectral-based techniques [20]. A taxonomy of graph types, training methods, and propagation processes was recently published in [142]. [139] categorized graph neural network advances as semi-supervised (graph convolution), unsupervised (graph auto-encoder), and latest advancements (graph recurrent neural network and graph reinforcement learning). Graph convolution, graph auto-encoder, graph recurrent neural network, and spatial-temporal graph neural networks are all included in [124]. These existing surveys, on the other hand, fail to integrate their categories into a cohesive framework.

There also exist many surveys about graph neural networks in a particular perspective. For example, a comprehensive and focused survey [67] was conducted on the field of graph neural networks with an attention mechanism. Another example [104] provided a perspective that several graph neural networks with negative sampling can be unified into a matrix factorization framework in an analytical form. Another similar work [80] proposed a general view demonstrating equivalent between network embedding approaches and matrix factorization by two objectives: one is for similar nodes, and the other is for distant nodes. One dedicated survey provided a unified paradigm for the systematic categorization and analysis on various existing heterogeneous network embeddings algorithms, creating four benchmark datasets with various properties and friendly interfaces for ten popular algorithms [130]. However, these works only focus on part of GNN family, lacking a universal perspective. Another way to understand GNN is building post-hoc models, and then identifying the underlying patterns in a statistical perspective [8, 68, 135]. This direction is since neural network is used without theories or domain knowledge. However, one potential downside is that post-hoc models may be biased, vulnerable to adversarial attacks, and hard to be verified. Our survey focus on interpretable graph neural network, which is based on solid theoretical support.

There are also other surveys on graph neural networks from various perspectives. For example, in the field of graph neural networks with an attention mechanism, a comprehensive and concentrated survey was undertaken [67]. Another example demonstrated how many graph neural networks with negative sampling might be merged into an analytical matrix factorization framework [104].

One similar study offered a general view proving that network embedding techniques and matrix factorization are equal in terms of two objectives: one for similar nodes and the other for distant nodes [80]. One specific survey created four benchmark datasets with diverse features and user-friendly interfaces for 10 common algorithms, providing a unified paradigm for systematic categorization and analysis on several existing heterogeneous network embeddings approaches [130]. However, these research are limited to a subset of the GNN family and lack a global perspective. Building post-hoc explainable models and then identifying the underlying patterns from a statistical standpoint is another technique to analyze GNN [8, 68, 135]. This is because neural networks are used without the usage of theories or domain expertise. However, post-hoc models have the potential to be biased, subject to adversarial attacks, and difficult to verify. Our research focuses on interpretable graph neural networks, which have a strong theoretical foundation.

In contrast to previous surveys, which either present independent categories in their taxonomies or only cover a few GNN in the literature, our proposed framework aims to bridge the gap between two major categories (i.e., spatial and spectral-based methods) and link all subcategories through strong theoretical support.

2 PROBLEM SETUP AND PRELIMINARY

Table 1. Commonly used notations

Notations	Descriptions
\mathcal{G}	A graph.
\mathbf{V}	The set of nodes in a graph.
\mathbf{E}	The set of edges in a graph.
$\mathbf{A}, \tilde{\mathbf{A}}$	The adjacency matrix and its normalization.
$\mathbf{L}, \tilde{\mathbf{L}}$	The graph Laplacian matrix and its normalization.
v	A node $v \in \mathbf{V}$.
e_{ij}	An edge $e_{ij} \in \mathbf{E}$.
$\lambda_i \in \Lambda$	Eigenvalue(s).
$\mathbf{U}, \mathbf{U}^\top$	Eigenvector matrix and its transpose.
$\mathbf{U}_i \in \mathbf{U}, \mathbf{u}^\top_i \in \mathbf{U}^\top$	Single eigenvector and its transpose.
\mathbf{D}	The degree matrix of \mathbf{A} and $\mathbf{D}_{ii} = \sum_{j=1}^n \mathbf{A}_{ij}$.
$\mathbf{X} \in \mathbf{R}^{N \times d}$	The feature matrix of a graph.
$\mathbf{Z} \in \mathbf{R}^{N \times b}$	New node feature matrix.
$\mathbf{H} \in \mathbf{R}^{N \times b}$	The node hidden feature matrix.
$\mathbf{h}_v \in \mathbf{R}^b$	The hidden feature vector of node v .
N	node number
b	dimension size of hidden feature
\odot	Element-wise product.
Θ, θ	Learnable model parameters.
$\mathbf{P}(\cdot), \mathbf{Q}(\cdot)$	Polynomial function.
$\mathcal{N}(v)$	Directed neighbors of node v

In this section, we outline basic concepts, necessary preliminary, and problem setup of learning node-level representation which is the major task in the GNN literature. A simple graph is defined as $\mathcal{G} = (\mathcal{V}, \mathcal{E})$, where \mathcal{V} is a set of n nodes and \mathcal{E} represents edges. An entry $v_i \in \mathcal{V}$ denotes a node, and $e_{i,j} = \{v_i, v_j\} \in \mathcal{E}$ indicates an edge between nodes i and j . The adjacency matrix

$\mathbf{A} \in \mathbb{R}^{N \times N}$ is defined by if there is a link between node i and j , $A_{i,j} = 1$, and else 0. Node features $\mathbf{X} \in \mathbb{R}^{N \times F}$ is a matrix with each entry $x_i \in \mathbf{X}$ representing the feature vector on node i . Another popular graph matrix is the graph Laplacian which is defined as $\mathbf{L} = \mathbf{D} - \mathbf{A} \in \mathbb{R}^{N \times N}$ where \mathbf{D} is the degree matrix. Due to its generalization ability [16], the symmetric normalized Laplacian is often used, which is defined as $\tilde{\mathbf{L}} = \mathbf{D}^{-\frac{1}{2}} \mathbf{L} \mathbf{D}^{-\frac{1}{2}}$. Another option is random walk normalization: $\tilde{\mathbf{L}} = \mathbf{D}^{-1} \mathbf{L}$. Note that normalization could also be applied to the adjacency matrix, and their relationship is $\tilde{\mathbf{L}} = \mathbf{I} - \tilde{\mathbf{A}}$.

Most GNNs focus on node-level embeddings, learning how a graph signal is modified by a graph topology, and outputting a filtered feature as:

$$f : G, \mathbf{X} \rightarrow \mathbf{Z}, \quad (1)$$

where we aim to find a mapping which can integrate graph structure and original node features, generating a update node representation \mathbf{Z} . G represents the graph connectivity, and many options are available as listed in Table 2, and most popular are symmetric normalized graph matrices.

Table 2. Graph Representations

Notations	Descriptions
\mathbf{A}	Adjacency matrix
\mathbf{L}	Graph Laplacian
$\tilde{\mathbf{A}} = \mathbf{A} + \mathbf{I}$	Adjacency with self loop
$\mathbf{D}^{-1} \mathbf{A}$	Random walk row normalized adjacency
$\mathbf{A} \mathbf{D}^{-1}$	Random walk column normalized adjacency
$\mathbf{D}^{-1/2} \mathbf{A} \mathbf{D}^{-1/2}$	Symmetric normalized adjacency
$\tilde{\mathbf{D}}^{-1} \tilde{\mathbf{A}}$	Left renormalized adjacency, $\tilde{\mathbf{D}}_{ii} = \sum_j \tilde{\mathbf{A}}_{ij}$
$\tilde{\mathbf{A}} \tilde{\mathbf{D}}^{-1}$	Right renormalized
$\tilde{\mathbf{D}}^{-1/2} \tilde{\mathbf{A}} \tilde{\mathbf{D}}^{-1/2}$	Symmetric renormalized
$(\tilde{\mathbf{D}}^{-1} \tilde{\mathbf{A}})^k$	Powers of left renormalized adjacency
$(\tilde{\mathbf{A}} \tilde{\mathbf{D}}^{-1})^k$	Powers of right renormalized adjacency

In this survey, we represent a graph using graph Laplacian or adjacency matrix, since there is no experimental or theoretical evidence showing any consistent advantages of every single filter listed Table 2 [119]. This survey focuses on two major categories, i.e., spectral- and spatial-based graph neural networks (GNNs), and two related definitions are listed below for understanding this paper.

Definition 2.1 (Spatial Method). By integrating graph connectivity G and node features \mathbf{X} , the updated node representations (\mathbf{Z}) are defined as:

$$\mathbf{Z} = f(G) \mathbf{X}, \quad (2)$$

where G is often implemented with \mathbf{A} or \mathbf{L} in existing works. Therefore, spatial methods focus on finding a **node aggregation function** $f(\cdot)$ that learns how to aggregate node features to obtain a updated node embedding \mathbf{Z} .

Before introducing another definition, the necessary preliminary background is offered: **(1) graph Fourier transform:** The graph Laplacian \mathbf{L} can be diagonalized [112, 147] as $\tilde{\mathbf{L}} = \mathbf{U} \mathbf{\Lambda} \mathbf{U}^\top$, where $\mathbf{\Lambda}$ is the diagonal matrix whose diagonal elements are the corresponding eigenvalues (i.e., $\Lambda_{ii} = \lambda_i$), and \mathbf{U} is also called eigenvectors. Further, the graph Fourier transform of a signal \mathbf{X} is

defined as $\hat{\mathbf{X}} = \mathbf{U}^\top \mathbf{X} \in \mathbb{R}^{N \times N}$ and its inverse as $\mathbf{X} = \mathbf{U} \hat{\mathbf{X}}$. **(2) spectral convolution:** According to the Convolution Theorem [97], the convolution is defined in the Fourier domain such that

$$f_1 * f_2 = \mathbf{U} [(\mathbf{U}^\top f_1) \odot (\mathbf{U}^\top f_2)],$$

where \odot is the element-wise product, and f_1/f_2 are two signals defined on the time or spatial domain.

Definition 2.2 (Spectral Method). A node signal $f_2 = \mathbf{X}$ is filtered by spectral function $\mathbf{g} = \mathbf{U}^\top f_1$ as:

$$\mathbf{g} * \mathbf{X} = \mathbf{U} [\mathbf{g}(\Lambda) \odot (\mathbf{U}^\top \mathbf{X})] = \mathbf{U} \text{diag}(\mathbf{g}(\Lambda)) \mathbf{U}^\top \mathbf{X}, \quad (3)$$

where \mathbf{g} is known as **frequency response function**. If \mathbf{g} is polynomial or rational function, then we can reduce the equation above to:

$$\mathbf{g} * \mathbf{X} = \mathbf{g}(\tilde{\mathbf{L}}) \mathbf{X}. \quad (4)$$

In short, the objective of spectral methods is to learn a function $\mathbf{g}(\cdot)$.

The aim is to use the data to learn how to approximate node aggregation or a frequency response function. Approximation theory is a branch of mathematics concerned with determining how functions can be best approximated using simpler functions and quantifying the faults introduced as a result. Polynomial or rational approximations are commonly used for this. Although polynomials are more known and comfortable, and rational functions appear complex and specialized, rational functions are more powerful at approximating functions near singularities and on unbounded domains than polynomials. In complex analysis literature, the basic features of rational functions are described. [3, 5, 18, 30, 87, 98, 101, 103, 106, 114, 149]. As a popular and important polynomial approximation, Chebyshev approximation is first introduced as spectral filter for graph convolution: A real symmetric graph Laplacian \mathbf{L} can be decomposed as $\mathbf{L} = \mathbf{U} \Lambda \mathbf{U}^{-1} = \mathbf{U} \Lambda \mathbf{U}^\top$. Chebyshev approximation on spectral filter \mathbf{g} is applied [35, 49] so that it can be approximated with a polynomials with order k :

$$\begin{aligned} \mathbf{g} * \mathbf{X} &= \mathbf{U} \mathbf{g}(\Lambda) \mathbf{U}^\top \mathbf{X} \\ &\approx \mathbf{U} \sum_k \theta_k T_k(\tilde{\Lambda}) \mathbf{U}^\top \mathbf{X} && (\tilde{\Lambda} = \frac{2}{\lambda_{\max}} \Lambda - \mathbf{I}_N) \\ &= \sum_k \theta_k T_k(\tilde{\mathbf{L}}) \mathbf{X} && (\mathbf{U} \Lambda^k \mathbf{U}^\top = (\mathbf{U} \Lambda \mathbf{U}^\top)^k) \end{aligned}$$

A most popular graph convolutional network [61] further simplifies this approximation by reducing the order to 1:

$$\begin{aligned} \mathbf{g} * \mathbf{X} &\approx \theta_0 \mathbf{I}_N \mathbf{x} + \theta_1 \tilde{\mathbf{L}} \mathbf{X} && (\text{expand to 1st order}) \\ &= \theta_0 \mathbf{I}_N \mathbf{x} + \theta_1 \left(\frac{2}{\lambda_{\max}} \mathbf{L} - \mathbf{I}_N \right) \mathbf{X} && (\tilde{\mathbf{L}} = \frac{2}{\lambda_{\max}} \mathbf{L} - \mathbf{I}_N) \\ &= \theta_0 \mathbf{I}_N \mathbf{x} + \theta_1 (\mathbf{L} - \mathbf{I}_N) \mathbf{X} && (\lambda_{\max}=2) \\ &= \theta_0 \mathbf{I}_N \mathbf{x} - \theta_1 \tilde{\mathbf{D}} \mathbf{A} \tilde{\mathbf{D}} \mathbf{X} && (\mathbf{L} = \mathbf{I}_N - \tilde{\mathbf{D}} \mathbf{A} \tilde{\mathbf{D}}) \\ &= \theta_0 (\mathbf{I}_N + \tilde{\mathbf{D}} \mathbf{A} \tilde{\mathbf{D}}) \mathbf{X} && (\theta_0 = -\theta_1) \\ &= \theta_0 (\tilde{\mathbf{D}}^{-\frac{1}{2}} \tilde{\mathbf{A}} \tilde{\mathbf{D}}^{-\frac{1}{2}}) \mathbf{x} && (\tilde{\mathbf{A}} = \mathbf{A} + \mathbf{I}_N, \tilde{\mathbf{D}}_{ii} = \sum_j \mathbf{A}_{ij}). \end{aligned}$$

Therefore, the only parameter to learn is θ_0 . In many other GNNs, the learnable parameters can be more or less depending the model configuration.

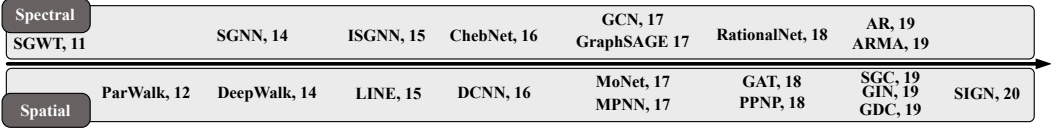


Fig. 1. Chronological overview of representative GNN.

3 FRAMEWORK OVERVIEW

Existing methods can be split into spatial and spectral-based methods depending on the type of graph neural networks. Several representative models are highlighted in Fig. 1. We can see that the spectral perspective is discussed earlier (SGWT [49], 2011), which forms the technical foundation of all the following spectral methods, including spectral convolution and approximation. Researchers continue to contribute to this thread and show promising potential to handle graph (SGNN [21], ISGNN [50], ChebNet [35]). Further, GCN [61], and GraphSAGE [47] design efficient training strategies, attracting considerable attention in the literature and researchers from different communities. After that, research in spectral methods was slowed except several works on rational filtering (RationalNet [27], AR [74], ARMA [12]). Meanwhile, attention is transferred to the spatial domain which has been dominating GNN so far. Early works in spatial methods are based on random walks (ParWalk [122], DeepWalk [100], LINE [113]) and CNN (DCNN [7]). After that, MPNN [44] established message-passing mechanism firmly in spatial methods. Polynomial approximation with high order has been discussed [63, 109, 121, 127], but still in the framework of ChebNet or DCNN. Note that many works discussed their proposed method in both spatial and spectral perspective [63, 92], but only cover few related works.

Different from existing surveys, we provide a way to comprehensively understand the spectral methods in the spatial perspective and vice versa for most GNNs. To merge spatial and spectral approaches into a coherent framework, a cross-domain perspective is introduced. As shown in Fig. 2, the proposed framework categorizes GNNs into the spatial (A-0) and spectral (B-0) domains, either of which is further divided into three subcategories (A-1/A-2/A-3 and B-1/B-2/B-3), respectively. Based on the types of node aggregation (i.e., f in Def. 2.1), A-0 is further divided into linear (A-1), polynomial (A-2) and rational (A-3) aggregations. Linear aggregation means only the first-order neighbors are involved, while polynomial aggregation considers high-order neighbors. Beyond them, rational aggregation adds reverse aggregation. B-0 is split into linear (B-1), polynomial (B-2), and rational (B-3) approximation based on the types of frequency filtering (i.e., g in Def. 2.2), since they explicitly belong to the approximation techniques. Each category and subcategory will be elaborated with examples in Section 4 and 5.

3.1 Inside the Spatial and Spectral Domain

This subsection shows the hierarchical relationship among the spatial and spectral domains, respectively. The spatial-based methods can be classified into three subcategories, and there are specialization and generalization relationship among them:

$$(A-1) \text{ LINEAR AGGREGATION} \rightleftarrows (A-2) \text{ POLYNOMIAL AGGREGATION} \rightleftarrows (A-3) \text{ RATIONAL AGGREGATION},$$

where it is a generalization from left to right, and specialization from right to left. Specifically, (A-1) summarizes all methods that linearly aggregate neighbors, i.e., learning a linear function among first-order neighbors, (A-2) contains approaches involving higher-order neighbors, and the order number is defined by the polynomials, and (A-3) covers aggregation with self-aggregation, which

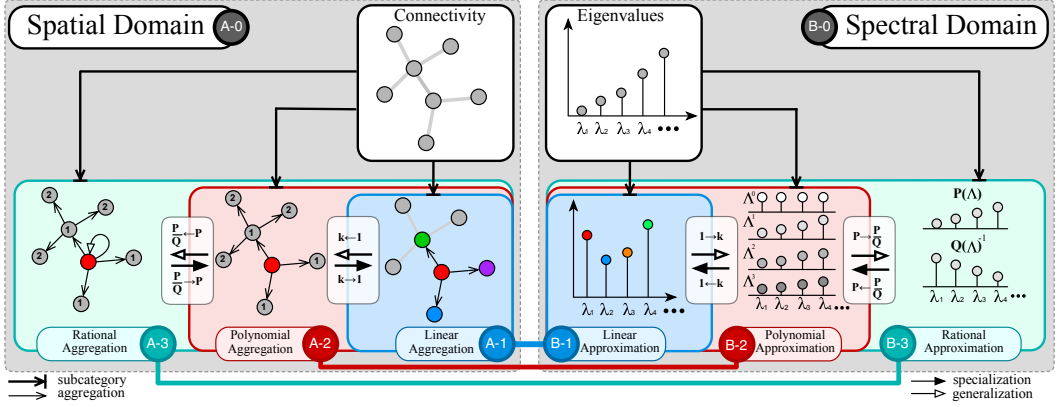


Fig. 2. Illustration of major graph neural operations and their relationship. Spatial and spectral methods are divided into three groups, respectively. Groups A-1, A-2, and A-3 are strongly-correlated by generalization and specialization, so are groups B-1, B-3, and B-3. The equivalence among them is marked in the same color.

is called rational aggregation. Therefore, (A-1) is generalized as (A-2) when involving higher-order neighbors, and (A-2) can be generalized as (A-3) after adding self-aggregation.

Similarly, the spectral-based methods are categorized into three subcategories:

$$(B-1) \text{ LINEAR APPROXIMATION} \rightleftharpoons (B-2) \text{ POLYNOMIAL APPROXIMATION} \rightleftharpoons (B-3) \text{ RATIONAL APPROXIMATION},$$

where it is a generalization from left to right, and specialization from right to left. Concretely, (B-1) outlines all models that aggregate frequency components using a linear function, while (B-2) uses polynomial approximation, and (B-3) includes rational approximation. Therefore, (B-1) can be generalized as (B-2) if replacing linear approximation with polynomial approximation, (B-2) is generalized as (B-3) if replacing polynomial approximation with rational approximation. Sections 3 and 4 will discuss details of these two threads respectively and exemplify using several graph neural networks.

3.2 Between the Spatial and Spectral Domain

In this subsection, we elaborate on the relationship across the boundary between the spatial and spectral domain. By transforming the analytical form of these subcategories, there is also equivalence as below. The first equivalence is between (A-1) and (B-1):

$$(A-1) \text{ LINEAR AGGREGATION} \rightleftharpoons (B-1) \text{ LINEAR APPROXIMATION},$$

which means that linear aggregation adjusting weights on neighbors corresponds to adjusting weights on frequency components using linear function in linear approximation. (A-1) and (B-1) can seamlessly convert to each other in closed form, and they have the same linear function. The only difference between (A-1) and (B-1) is that (A-1) models the target signal as a linear function of neighbor nodes, while (B-1) recovers the signal as a linear function of the frequency component. (A-2) and (B-2) are the same in terms of actual operation, i.e.,

$$(A-2) \text{ POLYNOMIAL AGGREGATION} \rightleftharpoons (B-2) \text{ POLYNOMIAL APPROXIMATION}.$$

This indicates that aggregating higher orders of neighbors in polynomial aggregation can be rewritten as the sum of different orders of frequency components in polynomial approximation. The last equivalence is

$$(A-3) \text{ RATIONAL AGGREGATION} \rightleftharpoons (B-3) \text{ RATIONAL APPROXIMATION},$$

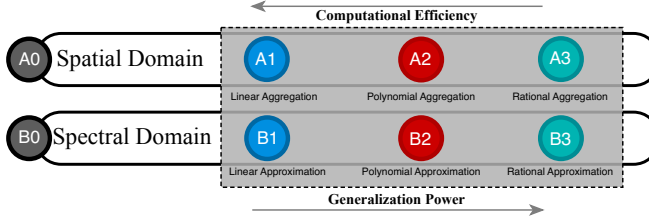


Fig. 3. Comparison of each category.

in which rational aggregation defines a label aggregation with self-aggregation, while rational approximation adjusts filter function with rational approximation. The comparison among these three pairs is provided below:

- **(A-1), (B-1):** This pair considers the first order neighbors (i.e., directed neighbors), and aggregates the representations of neighbors by tuning the weights of each neighbor. In spectral perspective, it applies linear filter function on eigenvalues with negative slope, i.e., $g(\lambda) = -\lambda + a$. This can be understood as low-pass filtering since the low-frequency components are assigned with higher weight by g than their original values (i.e., eigenvalues). The major advantage of this group is (1) its low computational cost and (2) many real-world scenarios subjects to *homophily* assumption (i.e., neighbors are similar). The main drawback is that homophily is not guaranteed in every network.
- **(A-2), (B-2):** Beyond the first order neighbors, this pair involves higher-order neighbors, which increases the capacity in modeling a more complex relationship among the neighborhood. In spectral perspective, it has theoretical superiority over (A-1)/(B-1), since (A-2)/(B-2) is a polynomial approximation as a spectral filter, while (A-1)/(B-1) is linear regression. Therefore, one shortcoming is also the price paid for border neighborhood and thereby higher computational complexity than (A-1)/(B-1). Another defect of this pair is the over-smoothing issue (i.e., all nodes are similar) if the order is set too large, and there is no golden rule regarding order size since it relies on the data. Note that K-layer (A-1) or (B-1) is equivalent to K-order of (A-2)/(B-2), so there is also an over-smoothing issue if stacking K-layer (A-1) or (B-1).
- **(A-3), (B-3):** To alleviate the over-smoothing issue, (A-3)/(B-3) introduce self-aggregation to limit the intensity of uni-directional aggregation in the spatial domain. This advantage can be explained in the spectral viewpoint as the superiority of rational approximation (A-3/B-3) over polynomial approximation (A-2/B-2). Specifically, the rational approximation is more powerful and accurate especially in estimating some abrupt signals such as discontinuity [3, 18, 30, 87, 101, 103, 114].

Therefore, we can summarize the pros and cons of each pair as shown in Fig. 3: there is a trade-off between computational efficiency and generalization power, so the category selection lies in the data complexity and the efficiency requirement. In the following section 4 and 5, representative GNN are analyzed with closed forms which are summarized in Table 3.

4 SPATIAL-BASED GNNS (A-0)

Spatial methods such as self-loop, normalization, high-order neighbors, aggregation, and combination of nodes are often discussed in the existing literature. Based on these operations, we have created a new taxonomy for spatial-based GNNs, classifying them into three distinct groups.

Table 3. Summary of Representative GNNs

	(A-0) Spatial-based	(B-0) Spectral-based
	Node Aggregation Function $f(\mathbf{A})$	Frequency Response Function $g(\Lambda)$
	(A-1) linear function of \mathbf{A}	(B-1) linear function of Λ
GCN	$\mathbf{I} + \tilde{\mathbf{A}}$	$2 - \Lambda$
GraphSAGE	$\hat{\mathbf{D}}^{-1} + \tilde{\mathbf{A}}$	$2 - \Lambda$
GIN	$(1 + \epsilon) \mathbf{I} + \mathbf{A}$	$2 + \epsilon - \Lambda$
	(A-2) polynomial function of \mathbf{A}	(B-2) polynomial function of Λ
ChebNet	$\phi \mathbf{I} + \sum_{i=1}^k \psi_i \tilde{\mathbf{A}}^i$	$\tilde{\theta}_0 \cdot 1 + \tilde{\theta}_1 \Lambda + \tilde{\theta}_2 \Lambda^2 + \dots$
DeepWalk	$\frac{1}{t+1} (\mathbf{I} + \tilde{\mathbf{A}} + \tilde{\mathbf{A}}^2 + \dots + \tilde{\mathbf{A}}^t)$	$\frac{1}{t+1} [\dots + \left((-1)^{t-1} + \binom{1}{t} \right) (-1)^{t-1}] + \dots]$
DCNN	$\psi_1 \tilde{\mathbf{A}} + \psi_2 \tilde{\mathbf{A}}^2 + \psi_3 \tilde{\mathbf{A}}^3 + \dots$	$\theta_1 \Lambda + \theta_2 \Lambda^2 + \theta_3 \Lambda^3 + \dots$
GDC	$\psi_1 \tilde{\mathbf{A}} + \psi_2 \tilde{\mathbf{A}}^2 + \psi_3 \tilde{\mathbf{A}}^3 + \dots$	$\theta_1 \Lambda + \theta_2 \Lambda^2 + \theta_3 \Lambda^3 + \dots$
Node2Vec	$\frac{1}{p} \mathbf{I} + \left(1 - \frac{1}{q} \right) \tilde{\mathbf{A}} + \frac{1}{q} \tilde{\mathbf{A}}^2$	$\left(1 + \frac{1}{p} \right) - \left(1 + \frac{1}{q} \right) \Lambda + \frac{1}{q} \Lambda^2$
LINE/SDNE	$\psi_1 \tilde{\mathbf{A}} + \psi_2 \tilde{\mathbf{A}}^2$	$\theta_1 \Lambda + \theta_2 \Lambda^2$
SGC	$0 \cdot \mathbf{I} + 0 \cdot \tilde{\mathbf{A}} + 0 \cdot \tilde{\mathbf{A}}^2 + \dots + 1 \cdot \tilde{\mathbf{A}}^K$	$\binom{K}{0} + \binom{K}{1} \Lambda^1 + \binom{K}{2} \Lambda^2 + \dots + \Lambda^n$
	(A-3) rational function of \mathbf{A}	(B-3) rational function of Λ
Auto-Regress	$\frac{1}{(1+\alpha) \mathbf{I} - \alpha \tilde{\mathbf{A}}}$	$\frac{1}{1+\alpha(1-\Lambda)}$
PPNP	$\frac{\alpha}{\mathbf{I} - (1-\alpha) \tilde{\mathbf{A}}}$	$\frac{\alpha}{\alpha \mathbf{I} + (1-\alpha) \Lambda}$
ARMA	$\frac{b}{(1-a) \tilde{\mathbf{A}}}$	$\frac{b}{(1-a+a\Lambda)}$
ParWalk	$\frac{\alpha}{\alpha \mathbf{I} + 1 - \tilde{\mathbf{A}}}$	$\frac{\beta}{\beta + \Lambda}$

4.1 Linear Aggregation (A-1)

A number of works [44, 47, 100, 115, 126, 127] fall into the category of learning the aggregation scheme among first order neighbors (i.e., direct neighbors). This aspect focuses on adjusting the weights for node and its first order neighbors to reveal the pattern regarding the supervision signal. Formally, each single updated node embeddings, $\mathbf{Z}(v_i)$, can be written as:

$$\mathbf{Z}(v_i) = \Phi(v_i) \mathbf{h}(v_i) + \sum_{u_j \in \mathcal{N}(v_i)} \Psi(u_j) \mathbf{h}(u_j), \quad (5)$$

where u_j denotes a neighbor of node v_i , $\mathbf{h}(\cdot)$ is their representations, and Φ/Ψ indicate the weight functions. The first item on the right hand side denotes the weighted representation of node v_i , while the second represents the update from its neighbors. By applying random walk normalization (i.e., dividing neighbors by degree of the current node), Eqn. (5) can be written as:

$$\mathbf{Z}(v_i) = \Phi(v_i) \mathbf{h}(v_i) + \sum_{u_j \in \mathcal{N}(v_i)} \Psi(u_j) \frac{\mathbf{h}(u_j)}{d_i}, \quad (6)$$

or by applying symmetric normalization, it can be written as:

$$\mathbf{Z}(v_i) = \Phi(v_i) \mathbf{h}(v_i) + \sum_{u_j \in \mathcal{N}(v_i)} \Psi(u_j) \frac{\mathbf{h}(u_j)}{\sqrt{d_i d_j}}, \quad (7)$$

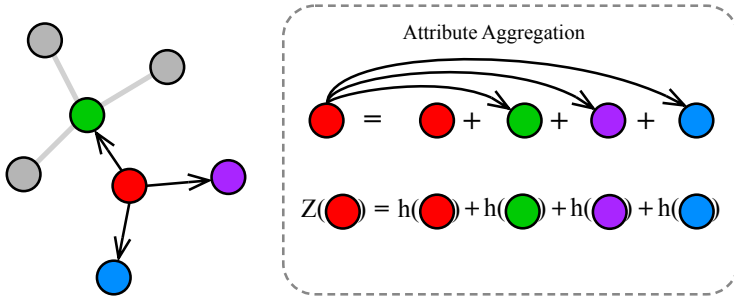


Fig. 4. Illustration of A-1

where d_i represents the degree of node v_i . Normalization has better generalization capacity, which is not only due to some implicit evidence but also because of a theoretical proof on performance improvement [58]. In a simplified configuration, weights for the neighbors are the same and is a scalar value ψ , and so is the weight for self node ϕ . Therefore, they can be rewritten in matrix form as:

$$\mathbf{Z} = \phi \mathbf{X} + \psi \mathbf{D}^{-1} \mathbf{A} \mathbf{X} = (\phi \mathbf{I} + \psi \mathbf{D}^{-1} \mathbf{A}) \mathbf{X}, \quad (8)$$

or

$$\mathbf{Z} = \phi \mathbf{X} + \psi \mathbf{D}^{-\frac{1}{2}} \mathbf{A} \mathbf{D}^{\frac{1}{2}} \mathbf{X} = (\phi \mathbf{I} + \psi \mathbf{D}^{-\frac{1}{2}} \mathbf{A} \mathbf{D}^{\frac{1}{2}}) \mathbf{X}. \quad (9)$$

Eqn. (8) and (9) can be generalized as the same form:

$$\mathbf{Z} = (\phi \mathbf{I} + \psi \tilde{\mathbf{A}}) \mathbf{X}, \quad (10)$$

where $\tilde{\mathbf{A}}$ denotes normalized \mathbf{A} , which could be implemented by random walk or symmetric normalization. As shown in Fig. 4, the new representation of the current node (in red) is updated as the sum of the previous representations of itself and its neighbors. (A-1) may adjust the weights of the neighbors.

Several state-of-the-art methods selected to illustrate this schema are discussed as follows:

4.1.1 Graph Convolutional Network (GCN). As the one state of the art, GCN [61] adds a self-loop to nodes, and applies a *renormalization* trick which changes degree matrix from $\mathbf{D}_{ii} = \sum_j \mathbf{A}_{ij}$ to $\hat{\mathbf{D}}_{ii} = \sum_j (\mathbf{A} + \mathbf{I})_{ij}$. Specifically, GCN can be written as:

$$\mathbf{Z} = \hat{\mathbf{D}}^{-\frac{1}{2}} \hat{\mathbf{A}} \hat{\mathbf{D}}^{-\frac{1}{2}} \mathbf{X} = \hat{\mathbf{D}}^{-\frac{1}{2}} (\mathbf{I} + \mathbf{A}) \hat{\mathbf{D}}^{-\frac{1}{2}} \mathbf{X} = (\mathbf{I} + \tilde{\mathbf{A}}) \mathbf{X}, \quad (11)$$

where $\hat{\mathbf{A}} = \mathbf{A} + \mathbf{I}$, and $\tilde{\mathbf{A}}$ is normalized adjacency matrix with self-loop. Therefore, Eqn. (11) is equivalent to Eqn. (10) when setting $\phi = 0$ and $\psi = 1$ with the *renormalization* trick. Besides, GCN takes the sum of each node and average of its neighbors as new node embeddings. Note that the normalization of GCN is different from the others, but the physical meaning is the same.

4.1.2 GraphSAGE. Computing intermediate representations of each node and its neighbors, GraphSAGE [47] applies an aggregation among its neighbors. Take mean aggregator as example, it averages a node with its neighbors, i.e.,

$$\mathbf{Z}(v_i) = \text{MEAN}(\{\mathbf{h}(v_i)\} \cup \{\mathbf{h}(u_j), \forall u_j \in \mathcal{N}(v_i)\}), \quad (12)$$

where \mathbf{h} indicates the intermediate representation, and \mathcal{N} denotes the neighbor nodes. Eqn. (12) can be written in matrix form after implementing MEAN using symmetric normalization:

$$\mathbf{Z} = \mathbf{D}^{-\frac{1}{2}} (\mathbf{I} + \mathbf{A}) \mathbf{D}^{-\frac{1}{2}} \mathbf{X} = (\mathbf{I} + \tilde{\mathbf{A}}) \mathbf{X}, \quad (13)$$

which is equivalent to Eqn. (10) with $\phi = 1$ and $\psi = 1$. Note that the key difference between GCN and GraphSAGE is the normalization strategy: the former is symmetric normalization with renormalization trick, and the latter is random walk normalization.

4.1.3 Graph Isomorphism Network (GIN). Inspired by the Weisfeiler-Lehman (WL) test, GIN [127] develops conditions to maximize the power of GNN, proposing a simple architecture, Graph Isomorphism Network (GIN). With strong theoretical support, GIN generalizes the WL test and updates node representations as:

$$\mathbf{Z} = (1 + \epsilon) \cdot \mathbf{h}(v) + \sum_{u_j \in \mathcal{N}(v_i)} \mathbf{h}(u_j) = [(1 + \epsilon) \mathbf{I} + \mathbf{A}] \mathbf{X}, \quad (14)$$

which is equivalent to Eqn. (10) with $\phi = 1 + \epsilon$ and $\psi = 1$. Note that GIN dose not perform any normalization.

4.1.4 Graph Attention Model (GAT). GAT [115] applies attention mechanism by adjusting neighbors' weights, instead of using uniform weights in many related works:

$$\mathbf{Z} = (W_{att} \otimes \mathbf{A}) \mathbf{X}, \quad (15)$$

where $W_{att} \in \mathbb{R}^{N \times N}$ is a matrix, and calculated by a forward neural network $W_{att}(i, j) = f(\mathbf{h}_i, \mathbf{h}_j)$ with a pair of node representations as input. GAT can be treated as learning dynamic weight on the neighbors since their weights are not uniform. MoNet [92] is similar to GAT, since its update follows:

$$\mathbf{Z}(v) = \sum_{u \in \mathcal{N}(v)} w_j(\mathbf{u}(\mathbf{h}_i, \mathbf{h}_j)) \mathbf{h}_j, \quad (16)$$

where \mathbf{u} is a d-dimensional vector of pseudo-coordinates $\mathbf{u}(x, y)$, and

$$w_j(\mathbf{u}) = \exp\left(-\frac{1}{2} \left(\mathbf{u} - \boldsymbol{\mu}_j\right)^\top \boldsymbol{\Sigma}_j^{-1} \left(\mathbf{u} - \boldsymbol{\mu}_j\right)\right), \quad (17)$$

where $\boldsymbol{\mu}_j$ are learnable $d \times d$ and $d \times 1$ covariance matrix and mean vector of a Gaussian kernel, respectively. Let $W_{MoNet} = w(u(\cdot))$ as a weight function of a pair of node representations representation, then it is also a attention model:

$$\mathbf{Z} = (W_{MoNet} \otimes \mathbf{A}) \mathbf{X}, \quad (18)$$

These works do not consider updating nodes with their original representations, i.e., $\phi = 0$ and ψ is replaced with matrix parameter W in Eqn. (10). However, it is easy to extend them with self node.

4.2 Polynomial Aggregation (A-2)

To integrate richer structural information, several studies [7, 35, 45, 113, 121] involve higher orders of neighbors. Since direct neighbors (i.e., first-order neighbors) are not always sufficient for representing the surroundings of one node. However, it also brings an issue that excessive order usually averages all node representations, causing an over-smoothing issue and losing its focus on the local neighborhood [74]. This motivates many models to tune the aggregation scheme on different orders of neighbors. Therefore, proper constraint and flexibility of orders are critical for node representation. High order of neighbors has been proved to characterize challenging signals such as Gabor-like filters [2].

Define the shortest distance between node i and j as $d_G(i, j)$, and $\partial\mathcal{N}(i, \tau)$ to be the set of nodes j that satisfies $d_G(i, j) = \tau$, i.e., τ -order neighbors. Formally, this type of work can be written as:

$$\mathbf{Z}(v_i) = \Phi(v_i) \mathbf{h}(v_i) + \overbrace{\sum_{u_j \in \mathcal{N}(v_i, \tau=1)} \Psi^{(\tau=1)} \mathbf{h}(u_j)}^{\text{1st-order neighbor}} + \overbrace{\sum_{u_j \in \mathcal{N}(v_i, \tau=2)} \Psi^{(\tau=1)} \mathbf{h}(u_j) + \dots}^{\text{2nd-order neighbor}} + \overbrace{\sum_{u_j \in \mathcal{N}(v_i, \tau=k)} \Psi^{(\tau=k)} \mathbf{h}(u_j) + \dots}^{\text{k-th order neighbor}}, \quad (19)$$

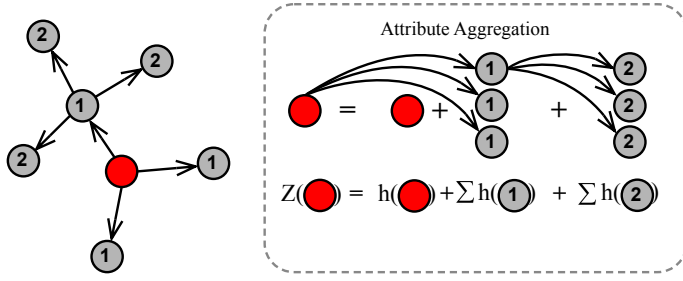


Fig. 5. Illustration of A-2.

where $\Psi^{(\tau)}$ indicates a scalar parameter for all τ -order neighbors. Setting the same order neighbors to share the same weights, Eqn. (19) can be rewritten in matrix form:

$$\mathbf{Z} = (\phi \mathbf{I} + \sum_{j=1}^k \psi_j \mathbf{A}^j) \mathbf{X} = \mathbf{P}_k(\mathbf{A}) \mathbf{X}, \quad (20)$$

where $\mathbf{P}_k(\cdot)$ is a polynomial function with order number k . Applying symmetric normalization, Eqn. (20) can be rewritten in matrix form as:

$$\mathbf{Z} = (\phi \mathbf{I} + \sum_{j=1}^k \psi_j (\mathbf{D}^{-\frac{1}{2}} \mathbf{A} \mathbf{D}^{-\frac{1}{2}})^j) \mathbf{X} = (\phi \mathbf{I} + \sum_{i=1}^k \psi_i \tilde{\mathbf{A}}^i) \mathbf{X} = (\sum_{i=0}^k \psi_i \tilde{\mathbf{A}}^i) \mathbf{X} = \mathbf{P}_k(\tilde{\mathbf{A}}) \mathbf{X}, \quad (21)$$

where $\phi = \psi_0$, and \mathbf{A} could also be normalized by random walk normalization: $\tilde{\mathbf{A}} = \mathbf{D}^{-1} \mathbf{A}$. As shown in Fig. 5, the new representation of the current node (in red) is updated as the sum of the previous representations of itself, its first and second-order neighbors. Note that the weights among those representations are learnable. Several existing works are analyzed below, showing that they are variants of Eqn. (20) or (21).

4.2.1 ChebNet. To bridge the gap, spectral convolutional operation is generalized, which requires expensive steps of spectral decomposition and matrix multiplication [39, 50]. Introducing truncated Chebyshev polynomial for estimating wavelet in graph signal processing, ChebNet [35] embeds a novel neural network layer for the convolution operator. Specifically, ChebNet can be written as:

$$\sum_{k=0}^{K-1} \theta_k T_k(\tilde{\mathbf{L}}) \mathbf{X} = (\tilde{\theta}_0 \mathbf{I} + \tilde{\theta}_1 \tilde{\mathbf{L}} + \tilde{\theta}_2 \tilde{\mathbf{L}}^2 + \dots) \mathbf{X}, \quad (22)$$

where $T_k(\cdot)$ denotes the Chebyshev polynomial and θ_k is the Chebyshev coefficient. $\tilde{\theta}$ is the coefficient after expansion and reorganization. Since $\tilde{\mathbf{L}} = \mathbf{I} - \tilde{\mathbf{A}}$, we have:

$$\sum_{k=0}^{K-1} \theta_k T_k(\tilde{\mathbf{L}}) \mathbf{X} = [\tilde{\theta}_0 \mathbf{I} + \tilde{\theta}_1 (\mathbf{I} - \tilde{\mathbf{A}}) + \tilde{\theta}_2 (\mathbf{I} - \tilde{\mathbf{A}})^2 + \dots] \mathbf{X}, \quad (23)$$

which can be reorganized as:

$$\sum_{k=0}^{K-1} \theta_k T_k(\tilde{\mathbf{L}}) \mathbf{X} = (\phi \mathbf{I} + \sum_{i=1}^k \psi_i \tilde{\mathbf{A}}^i) \mathbf{X} = \mathbf{P}_k(\tilde{\mathbf{A}}) \mathbf{X}, \quad (24)$$

which is exactly Eqn. (21). The predefined K is the order number of Chebyshev polynomial, and a larger K mean higher approximation accuracy in estimating the function of eigenvalues. Eqn. 24 shows that K also can be explained as the highest order of the neighbors.

4.2.2 DeepWalk . Applying random walk, DeepWalk [100] first draws a group of random paths from a graph and applies a skip-gram algorithm to extract node features. Assuming the number of random walk is large enough, the transition probability of random walk on a graph can be represented as:

$$\tilde{\mathbf{A}} = \mathbf{D}^{-1} \mathbf{A}. \quad (25)$$

Let the window size of skip-gram be $2t + 1$ and the current node is the $(t+1)$ -th one along each sampled random walk path, so the farthest neighbor current node can reach is the first one and the last one. A node and its neighbors are likely to appear in the same random walk path, and the neighbors follow the transition probability (Eqn. 25) to appear in the same path. Therefore, the updated representation is as follows:

$$\mathbf{Z} = \frac{1}{t+1} (\mathbf{I} + \tilde{\mathbf{A}} + \tilde{\mathbf{A}}^2 + \dots + \tilde{\mathbf{A}}^t) \mathbf{X} = \frac{1}{t+1} \mathbf{P}_k(\tilde{\mathbf{A}}) \mathbf{X}, \quad (26)$$

where \mathbf{I} means that DeepWalk always considers previous representation of the current node as one element, $\tilde{\mathbf{A}}$ represents the direct neighbors' transition probability, and $\tilde{\mathbf{A}}^2$ denotes that of the second-order neighbors. It will have at most t -order neighbors depending on the predefined length of the random walk (i.e., $2t + 1$).

4.2.3 Diffusion convolutional neural networks (DCNN). DCNN [7] uses a degree-normalized transition matrix (i.e., renormalized adjacency matrix: $\tilde{\mathbf{A}} = \tilde{\mathbf{D}} \mathbf{A}$) as graph representation, and performs node embedding update as:

$$\mathbf{Z} = \mathbf{W} \odot \tilde{\mathbf{A}}^* \mathbf{X} = [w_1, w_2, w_3, \dots, w_k]^\top \odot [\tilde{\mathbf{A}}, \tilde{\mathbf{A}}^2, \tilde{\mathbf{A}}^3, \dots, \tilde{\mathbf{A}}^k]^\top \mathbf{X}, \quad (27)$$

where $\tilde{\mathbf{A}}^*$ denotes a tensor containing the power series of $\tilde{\mathbf{A}}$, and the \odot operator represents element-wise multiplication. It can be transformed as:

$$\mathbf{Z} = (w_1 \tilde{\mathbf{A}} + w_2 \tilde{\mathbf{A}}^2 + w_3 \tilde{\mathbf{A}}^3 + \dots + w_k \tilde{\mathbf{A}}^k) \mathbf{X} = \mathbf{P}_k(\tilde{\mathbf{A}}) \mathbf{X}. \quad (28)$$

4.2.4 Scalable Inception Graph Neural Networks (SIGN). By generalizing GCN [61], GAT [115] and SGC [121], SIGN [109] constructs a block linear diffusion operators along with non-linearity. For node-wise classification tasks, SIGN has the form:

$$\begin{aligned} \mathbf{Z} &= \sigma([\mathbf{X}\Theta_0, \mathbf{A}_1\mathbf{X}\Theta_1, \dots, \mathbf{A}_r\mathbf{X}\Theta_r]), \\ \mathbf{Y} &= \xi(\mathbf{Z}\Omega), \end{aligned} \quad (29)$$

where $[\cdot, \cdot, \dots, \cdot]$ is concatenation, and r denotes the power number. Then, SIGN can be rewritten as:

$$\mathbf{Z} = [\mathbf{X}\Theta_0, \mathbf{A}_1\mathbf{X}\Theta_1, \dots, \mathbf{A}_r\mathbf{X}\Theta_r] \Omega = \omega_0\sigma(\mathbf{X}\Theta_0) + \omega_1\sigma(\mathbf{A}_1\mathbf{X}\Theta_1), \dots, \omega_r\sigma(\mathbf{A}_r\mathbf{X}\Theta_r), \quad (30)$$

where $\sigma(\mathbf{A}_r\mathbf{X}\Theta_r)$ could be treated as refined representation of each order of label aggregation by non-linear function σ and fully-connected layer Ω , i.e., $\widehat{\mathbf{A}^r \mathbf{X}}$. Replacing \mathbf{A} with normalized adjacency matrix, it can be rewritten as:

$$\hat{\mathbf{Z}} = \omega_0 \widehat{\tilde{\mathbf{A}}^0 \mathbf{X}} + \omega_1 \widehat{\tilde{\mathbf{A}}^1 \mathbf{X}} + \dots + \omega_r \widehat{\tilde{\mathbf{A}}^r \mathbf{X}} = \sum_r \omega_r \widehat{\tilde{\mathbf{A}}^r \mathbf{X}} = \widehat{\mathbf{P}(\tilde{\mathbf{A}}) \mathbf{X}}. \quad (31)$$

4.2.5 **Graph diffusion convolution (GDC)**. GDC [63] defines a generalized graph diffusion via the diffusion matrix:

$$\mathbf{Z} = \sum_{k=0}^{\infty} \theta_k \mathbf{T}^k, \quad (32)$$

where θ_k are the weighting coefficients with $\sum_{k=0}^{\infty} \theta_k = 1, \theta_k \in [0, 1], \mathbf{T}$ is a generalized undirected transition matrix which includes the random walk transition matrix $T_{rw} = \mathbf{A} \mathbf{D}^{-1}$, and the symmetric transition matrix $T_{sym} = \mathbf{D}^{-\frac{1}{2}} \mathbf{A} \mathbf{D}^{-\frac{1}{2}}$. In the general case, it can be written as :

$$\mathbf{Z} = \sum_{k=0}^{\infty} \theta_k \tilde{\mathbf{A}}^k = \mathbf{P}(\tilde{\mathbf{A}}). \quad (33)$$

4.2.6 **Node2Vec**. Node2Vec [45] defines a second-order random walk to control the balance between BFS (breath-first search) and DFS (depth-first search). Consider a random walk that traversed an edge between node t and v , denoted as (t, v) , and now it resides at node v . Then, the transition probabilities to next stop x from node t is defined as:

$$P(t \rightarrow x) = \begin{cases} \frac{1}{p} & \text{if } d(t, x) = 0, \text{ return to the source} \\ 1 & \text{if } d(t, x) = 1, \text{ BFS} \\ \frac{1}{q} & \text{if } d(t, x) = 2, \text{ DFS,} \end{cases} \quad (34)$$

where $d(t, x)$ denotes the shortest path between nodes t and x . $d(t, x)=0$ indicates a second-order random walk returns to its source node, (i.e., $t \rightarrow v \rightarrow t$), while $d(t, x)=1$ means that this walk goes to a BFS node, and $d(t, x)=2$ to a DFS node. The parameters p and q control the distribution of the three cases. Assuming the random walk is sufficiently sampled, Node2Vec can be rewritten in matrix form:

$$\mathbf{Z} = \left(\frac{1}{p} \cdot \overbrace{\mathbf{I}}^{\text{source}} + \overbrace{\tilde{\mathbf{A}}}^{\text{BFS}} + \frac{1}{q} \overbrace{(\tilde{\mathbf{A}}^2 - \tilde{\mathbf{A}})}^{\text{DFS}} \right) \mathbf{X}, \quad (35)$$

which can be transformed and reorganized as:

$$\mathbf{Z} = \left[\frac{1}{p} \mathbf{I} + \left(1 - \frac{1}{q}\right) \tilde{\mathbf{A}} + \frac{1}{q} \tilde{\mathbf{A}}^2 \right] \mathbf{X} = \mathbf{P}_{k=2}(\tilde{\mathbf{A}}) \mathbf{X}, \quad (36)$$

where transition probabilities $\tilde{\mathbf{A}} = \mathbf{D}^{-1} \mathbf{A}$ is random walk normalized adjacency matrix.

4.2.7 **LINE[77] / SDNE[118]**. These two models consider first order and second-order neighbors as the constraints for learning node embeddings. first order: the nodes representation is forced to be similar to its neighbors, which is equivalent to:

$$\mathbf{Z} = \tilde{\mathbf{A}} \mathbf{X}. \quad (37)$$

Second-order: the pair of nodes are forced to be similar if their neighbors are similar, which is equivalent to make second-order neighbors similar, therefore we can get the second-order connectivity by taking the power of the original adjacency:

$$\mathbf{Z} = \tilde{\mathbf{A}}^2 \mathbf{X}. \quad (38)$$

Then the final learned node embeddings are formulated as:

$$\mathbf{Z} = \tilde{\mathbf{A}} \mathbf{X} + \alpha \tilde{\mathbf{A}}^2 \mathbf{X} = \mathbf{P}_{k=2}(\tilde{\mathbf{A}}) \mathbf{X}. \quad (39)$$

Since LINE uses concatenation between the representations constrained by first and second-order, $\alpha = 1$; For SDNE, α is pre-defined.

4.2.8 Simple Graph Convolution (SGC). To reduce the computational overhead, SGC [121] removes non-linear function between neighboring graph convolution layers, and combines graph aggregation in one single layer:

$$\mathbf{Z} = \tilde{\mathbf{A}}^k \mathbf{X} \quad (40)$$

where $\tilde{\mathbf{A}}$ is renormalized adjacency matrix, i.e., $\tilde{\mathbf{A}} = \tilde{\mathbf{D}}^{-\frac{1}{2}} \mathbf{A} \tilde{\mathbf{D}}^{-\frac{1}{2}}$, where $\tilde{\mathbf{D}}^{-\frac{1}{2}}$ is degree matrix with self loop. Therefore, it can be easily rewritten as:

$$\mathbf{Z} = (0 \cdot \mathbf{I} + 0 \cdot \tilde{\mathbf{A}} + 0 \cdot \tilde{\mathbf{A}}^2 + \dots + 1 \cdot \tilde{\mathbf{A}}^k) \mathbf{X} = \mathbf{P}_k(\tilde{\mathbf{A}}) \mathbf{X}, \quad (41)$$

which only has the highest order term.

4.3 Rational Aggregation (A-3)

Most works merely consider label propagation from the node to its neighbors (i.e., gathering information from its neighbors) but ignore self-aggregation. Self-aggregation means that labels or attributes can be propagated back to itself or restart propagating with a certain probability. This reverse behavior can avoid over-smoothing issue [62]. Note that [A-2] can also alleviate over-smoothing issue by manually adjusting the order number, while [A-3] can do it automatically. Several works explicitly or implicitly implement self-aggregation by applying rational function on the adjacency matrix [12, 27, 57, 62, 69, 75, 83].

Since general label propagation is implemented by multiplying graph Laplacian, self-aggregation could be implemented by multiplying inverse graph Laplacian as:

$$\mathbf{Z} = \mathbf{P}_m(\tilde{\mathbf{A}}) \mathbf{Q}_n(\tilde{\mathbf{A}})^{-1} \mathbf{X} = \frac{\mathbf{P}_m(\tilde{\mathbf{A}})}{\mathbf{Q}_n(\tilde{\mathbf{A}})} \mathbf{X}, \quad (42)$$

where \mathbf{P} and \mathbf{Q} are two different polynomial functions, and the bias of \mathbf{Q} is often set to 1 to normalize the coefficients. As shown in Fig. 6, the new representations of the current node (in red) are updated as the previous one with probability \mathbf{P} , and as that of neighbors with probability $(1-\mathbf{P})$. The difference of A-3 beyond A-2 is that A-3 can avoid over-smoothing issue in an automatic manner [74, 140]. Over-smoothing issue happens when GNNs go deep, which would drive node features to a stationary point and average all the information from raw node representations. Graph convolution can be described as an optimization problem [75, 94, 140, 145], e.g., (1) minimizing the supervised loss and (2) keeping the local neighborhood similar:

$$\mathbf{Z} = \arg \min_{\mathbf{Z}} \left\{ \underbrace{\|\mathbf{Z} - \mathbf{Y}\|_2^2}_{(1) \text{ supervised loss}} + \alpha \underbrace{\text{Tr}(\mathbf{Z}^\top \mathbf{L} \mathbf{Z})}_{(2) \text{ neighborhood regularization}} \right\}, \quad (43)$$

where α is the controlling weight between the two constraints. The problem has analytical solution:

$$\mathbf{Z} = (\mathbf{I} + \alpha \tilde{\mathbf{L}})^{-1} \mathbf{Y} = ((1 + \alpha) \mathbf{I} - \tilde{\mathbf{A}}) \mathbf{Y}. \quad (44)$$

However, by repeatedly applying graph convolution multiple times, α increases thus it is prone to over-smoothing. Several different methods are proposed to solve the over-smoothing issue [25, 53, 108, 109, 128], and A-3 does so by keeping part of the original representation no matter how many iterations it performs, and thereby significantly reduces the over-smoothing issue.

4.3.1 Auto-Regressive. Label propagation (LP) [10, 141, 146] is a widely used methodology for graph-based learning. The objective of LP is two-fold: one is to extract embeddings that match with the node label, the other is to become similar to neighboring vertices. The label can be treated as part of node attributes, so we have:

$$\mathbf{Z} = (\mathbf{I} + \alpha \tilde{\mathbf{L}})^{-1} \mathbf{X} = \frac{\mathbf{I}}{\mathbf{I} + \alpha(\mathbf{I} - \tilde{\mathbf{A}})} \mathbf{X} = \frac{\mathbf{I}}{(1 + \alpha) \mathbf{I} - \alpha \tilde{\mathbf{A}}} \mathbf{X}, \quad (45)$$

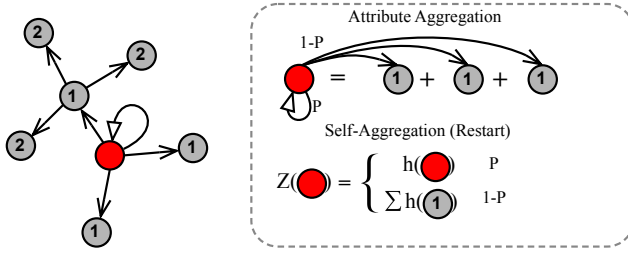


Fig. 6. Illustration of A-3.

which is the closed-form solution and also equivalent to the form of Eqn. (42), i.e., $\mathbf{P} = \mathbf{I}$ and $\mathbf{Q} = (1 + \alpha) \mathbf{I} - \alpha \tilde{\mathbf{A}}$.

4.3.2 Personalized PageRank (PPNP). Obtaining node's representation via teleport (restart), PPNP [15, 62, 133] keeps the original representation (self-aggregation) \mathbf{X} with probability α . Therefore, $1-\alpha$ is the probability of performing the normal label propagation:

$$\mathbf{Z} = \alpha \left(\mathbf{I} - (1 - \alpha) \tilde{\mathbf{A}} \right)^{-1} \mathbf{X} = \frac{\alpha}{\mathbf{I} - (1 - \alpha) \tilde{\mathbf{A}}} \mathbf{X}, \quad (46)$$

where $\tilde{\mathbf{A}} = \mathbf{D}^{-1} \mathbf{A}$ is random walk normalized adjacency matrix with self-loop. Eqn. (46) is with a rational function whose numerator is a constant.

4.3.3 ARMA filter [12]. ARMA filter approximates any desired filter response function with updates as:

$$\mathbf{Z} = \frac{b}{\mathbf{I} - a \tilde{\mathbf{A}}} \mathbf{X}. \quad (47)$$

Note that ARMA filter is an unnormalized version of PPNP. When $a+b=1$, ARMA becomes PPNP.

4.3.4 ParWalks. [74, 122] A partially absorbing random walk is a second-order Markov chain with partial absorption at each state. [122] also shows that with proper absorption, the absorption probabilities can well capture the global graph structure. Note that the concept "absorption" in [122] is similar to "teleport" or "restart" in PPNP [62]. ParWalks defines the aggregation as:

$$p_{ij} = \begin{cases} \frac{\alpha_i}{\alpha_i + d_i}, & i = j \\ \frac{w_{ij}}{\alpha_i + d_i}, & i \neq j, \end{cases} \quad (48)$$

where α is defined as a variable to control the level of absorption, w_{ij} and d_i indicate non-negative matrix of pairwise affinities between vertex i and j , and degree of vertex i , respectively.

$$\mathbf{Z} = \frac{\alpha \mathbf{I}}{\alpha + \tilde{\mathbf{L}}} \mathbf{X} = \frac{\alpha}{\alpha \mathbf{I} + \mathbf{I} - \tilde{\mathbf{A}}} \mathbf{X}, \quad (49)$$

where α is redefined as a regularizer in the original paper [122]. When $\alpha = 1$, all nodes follow the same absorbing behavior, otherwise each node has an independent absorbing policy. Also, ParWalks model is equivalent to ARMA filter ($a = b = \frac{1}{2}$) when $\alpha = 1$ and with normalized Laplacian:

$$\mathbf{Z} = \frac{\mathbf{I}}{\mathbf{I} + \tilde{\mathbf{L}}} \mathbf{X} = \frac{\mathbf{I}}{\mathbf{I} + (\mathbf{I} - \tilde{\mathbf{A}})} \mathbf{X} = \frac{\frac{1}{2} \mathbf{I}}{\mathbf{I} - \frac{1}{2} \tilde{\mathbf{A}}} \mathbf{X}. \quad (50)$$

The author also discussed the over-smoothing issue: when $\Lambda = \mathbf{I}$ and as $\alpha \rightarrow 0$, a ParWalk would converge to the constant distribution $1/n$, regardless of the starting vertex.

4.3.5 RationalNet. To leverage higher order of neighbors, RationalNet proposes a general rational function with predefined order number, and it is optimized by Remez algorithm. The analytic form is exactly Eqn. (42). The major difference beyond PPNP or ARMA filter is that RationalNet generalized them and the order can be any number.

Remark: The computational cost of A-3 is expensive since it involves the inverse of matrix. Typical solution is to apply iterative algorithms [12, 62, 69]. Note that we present one iteration or layer of Auto-Regression, PPNP, ARMA and ParWalks. Multiple iterations or layers make them higher orders.

4.4 Effect Analysis of Inverse Graph Laplacian in Graph Convolution

The major difference between rational and polynomial aggregation is whether there is polynomial of inverse graph Laplacian. The inverse of the graph Laplacian is a key object in online learning algorithms for graphs [51]. By leveraging the concept of conductance, with f as a heat distribution over the vertexes, $\mathbf{L}(f)$ indicates the flux induced by f over the graph. Then based on the representer theorem [6, 111], $f(\mathcal{V}_i) = \mathbf{L}^{-1}(\mathbf{L}(f))$ could be interpreted as the heat at each vertex been expressed concerning or derived from the flux through every vertex. Thus, when \mathbf{L} sends a heat distribution f over each node to flux through each vertex, \mathbf{L}^{-1} sends some of the fluxes over the graph back to the original heat distribution (i.e., keep part of fluxes itself). Going back to the graph learning application, we first translate our updated “heat distribution” to flux through all of those nodes by calculating $\mathbf{P}(\mathbf{L}(f))$. M-th degree of $\mathbf{P}(\cdot)$ means that each vertex can update M-th neighbors at most. Then using another updated flux in the reverse direction, $\mathbf{Q}(\mathbf{L}(f))^{-1}$ will adjust or reduce flux within N-th neighbors.

More layers or higher degree in polynomial aggregation tend to use more neighbors, thus increasing capacity. Many times, it is unavoidable to over-smooth when using too many layers or degrees (e.g., all nodes are similar). However, it is difficult to identify the optimal number of layers or degrees unless they are all tested. By contrast, ‘sending back’ (i.e., teleport) behavior of rational aggregation, in which the out-degree flux is limited even if excesses of graph convolutional layers or approximation degrees are added, completely overcomes the over-smoothing issue [62].

4.5 Connection among spatial methods

Three groups of spatial methods introduced above (i.e., A-1, A-2, A-3) are strongly connected under *generalization* and *specialization* relationship, as shown in Fig. (2):

- **Generalization:** *Linear Aggregation* can be extended to *Polynomial Aggregation* by adding more neighbors of higher order. *Polynomial Aggregation* can be upgraded to *Rational Aggregation* by adding reverse Aggregation;
- **Specialization:** *Linear Aggregation* is a special case of *Polynomial Aggregation* when setting the order to 1. *Polynomial Aggregation* is a special case of *Rational Aggregation* if removing reverse Aggregation.

5 SPECTRAL-BASED GNN (B-0)

Graph spectral theory involves the application of eigen-decomposition and analyzing the weight-adjusting function (i.e., frequency filter function or frequency response function) on eigenvalues of graph matrices. Frequency components (eigenvectors) are assigned weights in order to reconstruct the target signal by applying the filter’s output. We propose a new taxonomy of graph neural

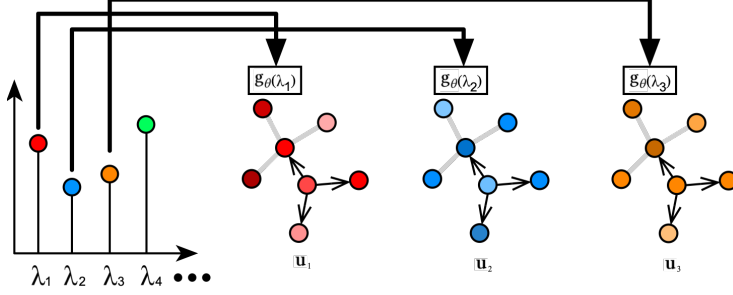


Fig. 7. Illustration of B-1.

networks, identifying three subgroups of spectral-based GNNs based on the type of the filter function.

5.1 Linear Approximation (B-1)

There exist numerous works that can be boiled down to adjusting weights of frequency components in the spectral domain. The goal of filter function is to adjust eigenvalues (i.e., the weights of eigenvectors) to fit the target output. Many of them are proven to be low-pass filters [75], which means that only low-frequency components are emphasized, i.e., the first few eigenvalues are enlarged, and the others are reduced. There exist a large number of works that can be understood as adjusting weights of frequency component during aggregation. Specifically, a linear function of g is employed:

$$\mathbf{Z} = \left(\sum_{i=0}^l \theta_i \lambda_i \mathbf{u}_i \mathbf{u}_i^T \right) \mathbf{X} = \mathbf{U} \mathbf{g}_\theta(\Lambda) \mathbf{U}^T \mathbf{X}, \quad (51)$$

where \mathbf{u}_i is the i -th eigenvector, and g is *frequency filter function* or *frequency response function* controlled by parameters θ , with selected l lowest frequency components. The goal of g is to change the weights of eigenvalues to fit the target output. As shown in Fig. 7, $A1$ updates the weights of eigenvectors ($\mathbf{u}_1, \mathbf{u}_2$) as $g_\theta(\lambda)$ which is a linear function. Several state-of-the-art methods introduced in the last section are analyzed to provide a better understanding of this scheme.

5.1.1 Graph Convolutional Network (GCN). Rewriting GCN [61] in spectral domain, we have:

$$\mathbf{Z} = \tilde{\mathbf{A}} \mathbf{X} = \mathbf{D}^{-\frac{1}{2}} (\mathbf{A} + \mathbf{I}) \mathbf{D}^{-\frac{1}{2}} \mathbf{X} = \mathbf{D}^{-\frac{1}{2}} (\mathbf{D} - \mathbf{L} + \mathbf{I}) \mathbf{D}^{-\frac{1}{2}} \mathbf{X} = (\mathbf{I} - \mathbf{L} + \mathbf{I}) \mathbf{D}^{-\frac{1}{2}} \mathbf{X} = \mathbf{U} (2 - \Lambda) \mathbf{U}^T \mathbf{X}, \quad (52)$$

where $\tilde{\mathbf{A}} = \mathbf{D}^{-\frac{1}{2}} (\mathbf{A} + \mathbf{I}) \mathbf{D}^{-\frac{1}{2}}$ is renormalization of $\tilde{\mathbf{A}}$. Therefore, the frequency response function is $g(\Lambda) = 1 - \Lambda$ which is a low-pass filter, i.e., smaller eigenvalues which correspond to low frequency components are assigned with a larger value.

5.1.2 GraphSAGE. Considering the MEAN aggregation as example, we can rewrite GraphSAGE [47] in matrix form:

$$\mathbf{Z} = \mathbf{D}^{-\frac{1}{2}} (\mathbf{I} + \mathbf{A}) \mathbf{D}^{-\frac{1}{2}} \mathbf{X} = (\mathbf{I} + \tilde{\mathbf{A}}) \mathbf{X} = (2\mathbf{I} - \tilde{\mathbf{L}}) \mathbf{X} = \mathbf{U} (2 - \Lambda) \mathbf{U}^T \mathbf{X}. \quad (53)$$

Hence, the frequency response function is $g(\Lambda) = 2 - \Lambda$ which is a low-pass filtering. Note that GraphSAGE's normalization is different from GCN, which utilizes the renormalization trick.

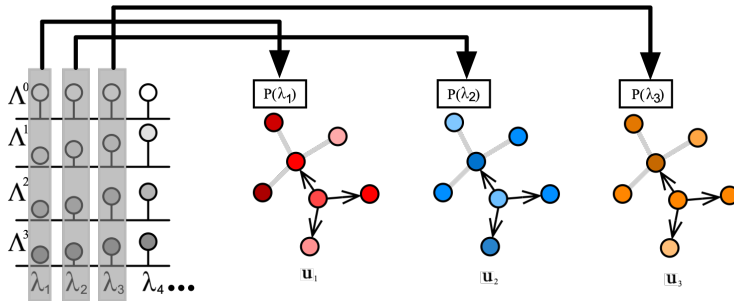


Fig. 8. Illustration of B-2.

5.1.3 **Graph Isomorphism Network (GIN).** Multi-Layer neural network is capable of fit the scale (i.e., normalization) [61], so GIN [127] can be rewritten as:

$$\mathbf{Z} = \mathbf{D}^{-\frac{1}{2}} [(1 + \epsilon) \mathbf{I} + \mathbf{A}] \mathbf{D}^{-\frac{1}{2}} \mathbf{X} = \mathbf{D}^{-\frac{1}{2}} [(2 + \epsilon) \mathbf{I} - \tilde{\mathbf{L}}] \mathbf{D}^{-\frac{1}{2}} \mathbf{X} = \mathbf{U}(2 + \epsilon - \Lambda) \mathbf{U}^T \mathbf{X}. \quad (54)$$

GIN can be seen as a generalization of GCN or GraphSAGE without normalized adjacency matrix \mathbf{A} . The frequency response function is $\mathbf{g}(\Lambda) = 2 + \epsilon - \Lambda$ which is low-pass.

5.1.4 **Summary.** The aforementioned methods apply linear low-pass filtering, and the only difference among them is that the bias is different (i.e., 2 for GCN, 2 for GraphSAGE, and $2 + \epsilon$ for GIN). Therefore, we study the influence of bias on the filter function, and define a metric:

$$w(\lambda_i) = \frac{|\text{bias} - \lambda_i|}{\sum_j |\text{bias} - \lambda_j|}, \quad (55)$$

which indicates the overall proportion change of each eigenvalue after applying response function. A large adjusted value means that the filtering will enlarge the influence of corresponding eigenvector. The range of the eigenvalue is in $[0, 2)$ for the normalized Laplacian matrix [29]. If let *bias* be larger or equal than 2, we have:

$$w(\lambda_i) = \frac{\text{bias} - \lambda_i}{N \cdot \text{bias} - \sum_j \lambda_j} = \overbrace{\frac{-1}{N \cdot \text{bias} - \sum_j \lambda_j}}^{\text{slope}} \lambda_i + \overbrace{\frac{\text{bias}}{N \cdot \text{bias} - \sum_j \lambda_j}}^{\text{intercept}}, \quad (56)$$

when *bias* is larger or equal than 2, the slope is positive, which means that the filter function is high-pass. As the bias increases, the slope becomes larger, which means that larger weights are assigned to high-frequency spectral components. Also, all adjusted values by the filter function are positive, while negative weights are difficult to interpret.

5.2 Order of Approximation (B-2)

Considering higher order of frequency, filter function can approximate any smooth filter function, because it is equivalent to applying the polynomial approximation. Therefore, introducing higher-order of frequencies boosts the representation power of filter function in simulating spectral signal. Formally, this type of work can be written as:

$$\mathbf{Z} = \left(\sum_{i=0}^l \sum_{j=0}^k \theta_j \lambda_i^j \mathbf{u}_i \mathbf{u}_i^T \right) \mathbf{X} = \mathbf{U} \mathbf{P}_\theta(\Lambda) \mathbf{U}^T \mathbf{X}, \quad (57)$$

where $\mathbf{g}(\cdot) = \mathbf{P}_\theta(\cdot)$ is a polynomial function.

As shown in Fig. 8, A2 updates the weights of eigenvectors ($\mathbf{u}_1, \mathbf{u}_2$) as $\mathbf{P}_\theta(\lambda)$ which is a polynomial function.

5.2.1 **ChebNet**. As analyzed in Eq. 24, ChebNet [49] can be written as:

$$\sum_{k=0}^{K-1} \theta_k T_k(\tilde{\mathbf{L}}) \mathbf{X} = (\tilde{\theta}_0 \mathbf{I} + \tilde{\theta}_1 \tilde{\mathbf{L}} + \tilde{\theta}_2 \tilde{\mathbf{L}}^2 + \dots) \mathbf{X}, \quad (58)$$

where $T_k(\cdot)$ is the Chebyshev polynomial and θ_k is the Chebyshev coefficient. $\tilde{\theta}$ is the coefficient after expansion and reorganization. Therefore, we can rewrite it as:

$$\sum_{k=0}^{K-1} \theta_k T_k(\tilde{\mathbf{L}}) \mathbf{X} = \mathbf{U}(\tilde{\theta}_0 \cdot 1 + \tilde{\theta}_1 \Lambda + \tilde{\theta}_2 \Lambda^2 + \dots) \mathbf{U}^\top \mathbf{X}, \quad (59)$$

where spectral response function is $\mathbf{g}(\Lambda) = \tilde{\theta}_0 \cdot 1 + \tilde{\theta}_1 \Lambda + \tilde{\theta}_2 \Lambda^2 + \dots = \mathbf{P}(\Lambda)$.

5.2.2 **DeepWalk**. Starting from Eq. 26, DeepWalk [100] can be rewritten as:

$$\begin{aligned} \mathbf{Z} &= \frac{1}{t+1} (\mathbf{I} + \tilde{\mathbf{A}} + \tilde{\mathbf{A}}^2 + \dots + \tilde{\mathbf{A}}^t) \mathbf{X} \\ &= \frac{1}{t+1} (\mathbf{I} + (\mathbf{I} - \tilde{\mathbf{L}}) + (\mathbf{I} - \tilde{\mathbf{L}})^2 + \dots + (\mathbf{I} - \tilde{\mathbf{L}})^t) \mathbf{X} \\ &= \frac{1}{t+1} (2\mathbf{I} + (-1 - 2 - 3 - \dots) \tilde{\mathbf{L}} + (1 + 3 + 6 + \dots) \tilde{\mathbf{L}}^2 + \dots + ((-1)^{t-1} + \binom{1}{t}) (-1)^{t-1} \tilde{\mathbf{L}}^{t-1} + (-1)^t \tilde{\mathbf{L}}^t) \mathbf{X} \\ &= (\theta_0 \mathbf{I} + \theta_1 \tilde{\mathbf{L}} + \theta_2 \tilde{\mathbf{L}}^2 + \dots + \theta_t \tilde{\mathbf{L}}^t) \mathbf{X} \\ &= \mathbf{U}(\theta_0 + \theta_1 \Lambda + \theta_2 \Lambda^2 + \dots + \theta_t \Lambda^t) \mathbf{U}^\top \mathbf{X} \\ &= \mathbf{U} \mathbf{P}_{k=r}(\Lambda) \mathbf{U}^\top \mathbf{X}, \end{aligned}$$

where $\mathbf{g}(\Lambda) = \theta_0 + \theta_1 \Lambda + \theta_2 \Lambda^2 + \dots + \theta_t \Lambda^t$, and all parameters θ_i are determined by the predefined step size t .

5.2.3 **Scalable Inception Graph Neural Networks (SIGN)**. Substituting $\tilde{\mathbf{A}} = \mathbf{I} - \tilde{\mathbf{L}}$ in Eq. 31, it can be rewritten as:

$$\hat{\mathbf{Z}} = \sum_r \omega_r \widehat{(\mathbf{I} - \tilde{\mathbf{L}})^r} \mathbf{X} = \mathbf{U} \widehat{\mathbf{P}_{k=r}(\Lambda)} \mathbf{X} \mathbf{U}^\top. \quad (60)$$

5.2.4 **Graph diffusion convolution (GDC)**. Substituting $\tilde{\mathbf{A}} = \mathbf{I} - \tilde{\mathbf{L}}$, general case in Eq. 33 can be written as:

$$\mathbf{Z} = \sum_{k=0}^{\infty} \theta_k (\mathbf{I} - \tilde{\mathbf{L}})^k = \mathbf{U} \sum_{k=0}^{\infty} \theta_k (1 - \Lambda)^k \mathbf{U}^\top = \mathbf{U} \mathbf{P}(\Lambda) \mathbf{X} \mathbf{U}^\top. \quad (61)$$

5.2.5 **Diffusion convolutional neural networks (DCNN)**. As analyzed in Eq. 27, DCNN [7] can be transformed with $\tilde{\mathbf{A}} = \mathbf{I} - \tilde{\mathbf{L}}$ as:

$$\mathbf{Z} = \mathbf{P}(\mathbf{I} - \tilde{\mathbf{L}}) \mathbf{X} = \mathbf{U} \mathbf{P}(\Lambda) \mathbf{X} \mathbf{U}^\top, \quad (62)$$

which is equivalent to ChebNet, and parameters θ_i are learnable.

5.2.6 **Node2Vec**. Node2Vec [45] can be rewritten in matrix form as Eq. 35. Then it can be transformed and reorganized after substituting $\tilde{\mathbf{A}} = \mathbf{I} - \tilde{\mathbf{L}}$:

$$\mathbf{Z} = \left[\left(1 + \frac{1}{p}\right) \mathbf{I} - \left(1 + \frac{1}{q}\right) \tilde{\mathbf{L}} + \frac{1}{q} \tilde{\mathbf{L}}^2 \right] \mathbf{X} = \mathbf{U} \left[\left(1 + \frac{1}{p}\right) - \left(1 + \frac{1}{q}\right) \Lambda + \frac{1}{q} \Lambda^2 \right] \mathbf{U}^\top \mathbf{X}. \quad (63)$$

Therefore, Node2Vec's frequency response function is:

$$\mathbf{g}(\Lambda) = \left(1 + \frac{1}{p}\right) - \left(1 + \frac{1}{q}\right) \Lambda + \frac{1}{q} \Lambda^2, \quad (64)$$

which integrates a second order function of Λ with predefined parameters, i.e., p and q .

5.2.7 **LINE/SDNE**. As described in Eq. 39, LINE [77] and SDNE [118] can be rewritten as:

$$\mathbf{Z} = \tilde{\mathbf{A}} \mathbf{X} + \alpha \tilde{\mathbf{A}}^2 \mathbf{X} = (\mathbf{I} - \tilde{\mathbf{L}}) \mathbf{X} + \alpha (\mathbf{I} - \tilde{\mathbf{L}})^2 \mathbf{X} = \mathbf{U} [(\mathbf{I} - \Lambda) + \alpha (1 - \Lambda)^2] \mathbf{X} \mathbf{U}^\top = \mathbf{U} \mathbf{P}_{k=2}(\Lambda) \mathbf{U}^\top \mathbf{X}, \quad (65)$$

where response function $\mathbf{g}(\Lambda) = \Lambda + \alpha \Lambda^2$ is a polynomial function with order 2.

5.2.8 **Simple Graph Convolution (SGC)**. As analyzed in Eq. 41, SGC can be transformed as:

$$\begin{aligned} \mathbf{Z} &= (\mathbf{I} - \tilde{\mathbf{L}})^k \mathbf{X} = \left[\binom{k}{0} \mathbf{I} + \binom{k}{1} \tilde{\mathbf{L}} + \binom{k}{2} \tilde{\mathbf{L}}^2 + \dots + \tilde{\mathbf{L}}^k \right] \mathbf{X} \\ &= \mathbf{U} \left[\binom{k}{0} + \binom{k}{1} \Lambda + \binom{k}{2} \Lambda^2 + \dots + \Lambda^k \right] \mathbf{U}^\top \mathbf{X}, \end{aligned}$$

where spectral response function is a polynomial function of order k :

$$\mathbf{g}(\Lambda) = \binom{k}{0} + \binom{k}{1} \Lambda + \binom{k}{2} \Lambda^2 + \dots + \Lambda^k.$$

5.2.9 **Improved GCN (IGCN)**. By stacking multiple layers IGCN [75] is proposed as:

$$\mathbf{Z} = \tilde{\mathbf{L}}^k \mathbf{X} = \mathbf{U} \Lambda^k \mathbf{U}^\top \mathbf{X}, \quad (66)$$

where the spectral response function is a polynomial function with order k .

Summary In theory, polynomial approximation becomes more accurate as the order increases [5, 30, 98, 103, 114]. Note that linear approximation (B-1) can be treated as a polynomial approximation with order of 1. We study polynomial approximation on $\text{sign}(x)$ function, showing the difference among all the examples listed in (B-2). As shown in Fig. 9(a), linear function cannot well approximate $\text{sign}(x)$, since it is difficult for any straight line to fit a jump signal. When applying polynomial approximation, the situation become much better as shown in Fig. 9(b). If increasing the order of polynomial function, the variance will significantly reduced (Fig. 9(c)). To summarize, higher-order polynomial approximation is more accurate, but it comes at the cost of increased computational complexity. Therefore, Node2Vec/LINE/SDNE with an order of 2 have relatively low approximation power than the those with more than 2 layers/orders (e.g., ChebNet, DeepWalk, Diffusion CNN, Simple Graph Convolution), since the order of the latter is predefined and could be as large as possible.

5.3 Approximation Type (B-3)

Despite the fact that polynomial approximation is frequently used and experimentally successful, it only works when applied to a smooth spectral signal. However, no real-world transmission can be

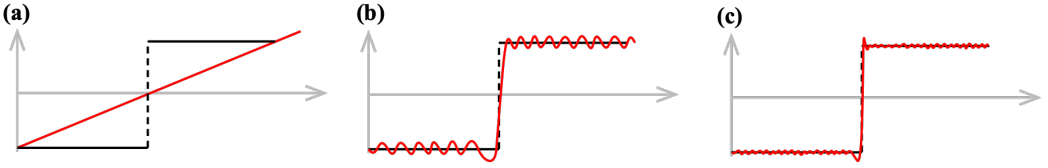


Fig. 9. Approximation for $\text{sign}(x)$: (a) linear approximation (b) polynomial approximation with low orders, (c) polynomial approximation with high orders.

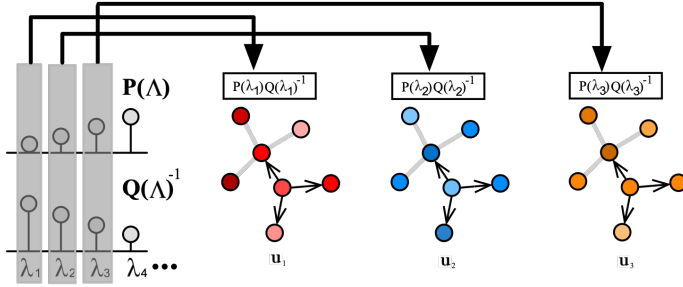


Fig. 10. Illustration of B-3.

guaranteed to be smooth. As a result, the rational approximation is used to increase non-smooth signal modeling accuracy. The following is an example of a rational kernel-based method:

$$\mathbf{Z} = \left(\sum_i^l \frac{\sum_{j=0}^k \theta_j \lambda_i^j}{\sum_{m=1}^n \phi_m \lambda_i^m + 1} \mathbf{u}_i \mathbf{u}_i^T \right) \mathbf{X} = \mathbf{U} \frac{\mathbf{P}_\theta(\Lambda)}{\mathbf{Q}_\phi(\Lambda)} \mathbf{U}^T \mathbf{X}, \quad (67)$$

where $\mathbf{g}(\cdot) = \frac{\mathbf{P}_\theta(\cdot)}{\mathbf{Q}_\phi(\cdot)}$ is a rational function, and \mathbf{P}, \mathbf{Q} are independent polynomial functions. Spectral methods process graph as a signal in the frequency domain. As shown in Fig. 10, A1 updates the weights of eigenvectors ($\mathbf{u}_1, \mathbf{u}_2$) as $\mathbf{g}_\theta(\lambda)$ which is a rational function.

5.3.1 Auto-Regressive filter. Label propagation (LP) [10, 141, 146] is a prevail methodology for graph-based learning. The objective of LP is two-fold: one is to extract embeddings that matches with the label, the other is to be similar with neighboring vertices. Label can be treated as part of node attributes, so we can have:

$$\mathbf{Z} = (\mathbf{I} + \alpha \tilde{\mathbf{L}})^{-1} \mathbf{X} = \mathbf{U} \frac{1}{1 + \alpha(1 - \Lambda)} \mathbf{U}^T \mathbf{X}. \quad (68)$$

5.3.2 PPNP. Personalized PageRank (PPNP) [62] can obtain node's representation via teleport (restart) probability α which indicates the ratio of keeping the original representation:

$$\mathbf{Z} = \frac{\alpha}{\mathbf{I} - (1 - \alpha)(\mathbf{I} - \tilde{\mathbf{L}})} \mathbf{X} = \mathbf{U} \frac{\alpha}{\alpha + (1 - \alpha)\Lambda} \mathbf{U}^T \mathbf{X}, \quad (69)$$

where $\tilde{\mathbf{A}} = \mathbf{D}^{-1} \mathbf{A}$ is random-walk normalized adjacency matrix with self-loop. Eq. 69 is with a rational function whose numerator is a constant.

5.3.3 **ARMA filter.** Substituting $\tilde{\mathbf{A}} = \mathbf{I} - \tilde{\mathbf{L}}$, Eq. 47 can be rewritten as:

$$\mathbf{Z} = \frac{b}{\mathbf{I} - a(\mathbf{I} - \tilde{\mathbf{L}})} \mathbf{X} = \mathbf{U} \frac{b}{(1-a) + a\Lambda} \mathbf{U}^T \mathbf{X}. \quad (70)$$

Note that ARMA filter is an unnormalized version of PPNP. When $a+b=1$, ARMA filter becomes PPNP. Therefore, ARMA filter is more generalized than PPNP due to its unnormalization.

5.3.4 **ParWalks.** [74, 122] Decomposing graph Laplacian, ParWalks can be written as:

$$\mathbf{Z} = \mathbf{U} \frac{\beta}{\beta + \Lambda} \mathbf{X} \mathbf{U}^T, \quad (71)$$

when setting $\beta = \frac{\alpha}{1-\alpha}$, it becomes PPNP:

$$\mathbf{Z} = \mathbf{U} \frac{\frac{\alpha}{1-\alpha}}{\frac{\alpha}{1-\alpha} + \Lambda} \mathbf{X} \mathbf{U}^T = \mathbf{U} \frac{\alpha}{\alpha + (1-\alpha)\Lambda} \mathbf{X} \mathbf{U}^T. \quad (72)$$

5.3.5 **RationalNet.** Substituting $\tilde{\mathbf{A}} = \mathbf{I} - \tilde{\mathbf{L}}$, Eq. 42 can be transform to Eq. 67. The frequency response function is a generalized rational function.

5.3.6 **Summary.** When the function to approximate contains discontinuities, rational function has overwhelming advantage over the polynomials or linear functions. Fig. 11 illustrates the difference between rational and polynomial approximation. Theoretically, rational approximation only needs exponentially less orders than that of polynomial functions [27].

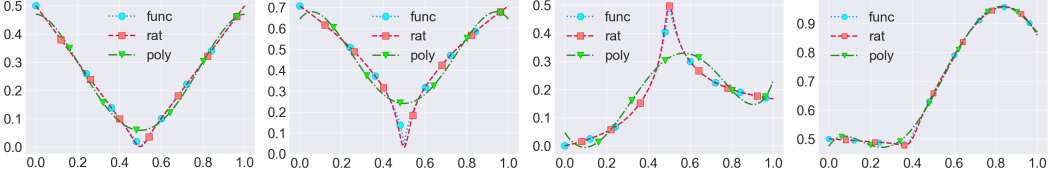


Fig. 11. Rational (rat) and polynomial (poly) approximation for several functions with discontinuity (func). From left to right: $\sqrt{|x-0.5|}$; $|x-0.5|$; $\frac{x}{10|x-0.5|+1}$; $\max(0.5, \sin(x+x^2)) - \frac{x}{20}$

5.4 Connection among spectral methods

There is a strong-tie among the aforementioned three groups of spectral methods in the perspective of *generalization* and *specialization*, as shown in Fig. (2):

- **Generalization:** *Linear Approximation* can be extended to *Polynomial Approximation* by adding more higher order of eigenvalues, i.e., $1 \leftarrow k$. *Polynomial Approximation* can be upgraded to *Rational Approximation* if the denominator of filter function is not 1;
- **Specialization:** *Linear Aggregation* is a special case of *Polynomial Approximation* by setting the highest order to 1. *Rational Approximation* is a special case of *Rational Approximation* by setting the denominator of filter function to 1.

6 THEORETICAL ANALYSIS

In terms of volume, spatial-based approaches outnumber spectrum-based methods in the literature [1, 20, 124, 139, 142], owing to the following reasons: (1) Spectral-based methods have a much higher computing overhead than spatial-based methods, and spectral methods are less intuitive than spatial methods. (2) Spatial-based approaches are convenient for model construction and

scalability. However, from a spatial and spectral perspective, there is a trade-off; neither has a major advantage over the other. This section describes several views of view and their benefits and drawbacks.

6.1 Uncertainty Principle: Global v.s. Local Perspectives

Spectral-based methods analyze graph filtering from spectral domain, decomposing signal into orthogonal frequency components. Each frequency represents a global basis: low-frequency components highlight the weights of neighborhood with low variance (i.e., little difference), while high-frequency components are associated with high variance in neighborhood. In other words, topological properties are reflected in the Laplacian spectrum: the first eigenvalues are associated with strong community structure, while the last eigenvalues reflect the bipartiteness of the graph [33, 34]. Left of Fig. 12 shows a typical low-pass filtering function on eigenvalues, which increases the small eigenvalues and decreases the adjusted values for large eigenvalues. In this case, only low-frequency components are kept, and neighbors have little variances. Spatial-based methods characterize filtering pattern from the local neighborhood. Most GNNs assume homophily among neighbors, so it is smooth or with little variance when walking through the neighborhood, which is exactly the same concept with low-pass filtering. Fig. 12 illustrates the relationship between a low-pass filtering in the spectral domain (left) and its effects in spatial domain (middle and right) [33]. Global and local perspectives are inconsistent on the surface, but they virtually describe the same signal in different ways when: (1) Low-pass/high-pass filtering in the spectral domain; (2) Neighbors are similar/dissimilar in the spatial domain.

However, it does not mean that the observations from the spatial/spectral domain or global/local perspectives are exactly equivalent. In quantum mechanics, the Heisenberg’s uncertainty principle [40] describe a limit to the accuracy for certain pairs of complementary variables or canonically conjugate variables of a particle, implying that predicting the value of a quantity with arbitrary certainty is impossible. Specifically,

$$\Delta_t^2 \Delta_\omega^2 \geq \frac{1}{4}, \quad (73)$$

where Δ_t and Δ_ω denote time spread and frequency spread, respectively. There is a trade-off between time concentration and frequency concentration for a signal. Inspired by quantum uncertainty principle, spectral graph analogy is developed [4], showing a trade-off between a signal’s localization on a graph and in its spectral domain. By quantifying spreads in the vertex ($\Delta_{g,u_0}^2(\mathbf{x})$) and spectral domain ($\Delta_s^2(\mathbf{x})$) of a graph signal \mathbf{x} , a lower bound on the product of the two spreads is identified. This conclusion indicates that there is no better method between the spatial-based and spectral-based GNNs: applying spatial-based GNNs will lose part of accuracy in the spectral domain, and spectral-based GNNs will also lose spatial accuracy. In sum:

- **Global and local perspectives are strong connected:** global observation is generalization of local situations, while details from local perspective embodies the global statistics.
- **Global and local perspectives outperform each other in their own domains:** high resolution in global loses details in local perspective, and more details in local observations blur the global viewpoint.

Therefore, several existing works bridge this information gap between global and local perspectives, or spectral and spatial information, to enhance the expressive capacity of GNNs [14, 76, 116, 138, 144, 148]. Based on the analysis above, we can safely conclude that there is no perfect modeling on global or local perspectives, but can only have a proper trade-off between them. As shown in Table 4, four aspects are compared:

Table 4. Comparison between the Spatial (A-0) and Spectral (B-0) Methods

	Methodology	Computation	Space Complexity	Stability
Spectral	Global	One-step	High	Exact
Spatial	Local	Iterative	Low	Approximate

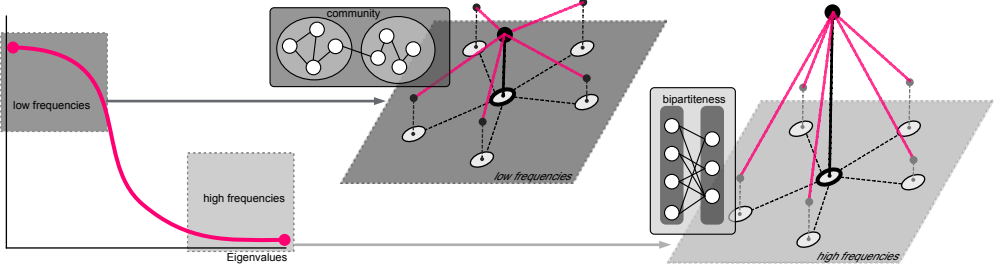


Fig. 12. Connection between the Spatial and Spectral Perspective

Table 5. Comparison on Time Complexity and Expressive Power

	Linear (A-1/B-1)	Polynomial (A-2/B-2)	Rational (A-3/B-3)
Time	$\mathcal{O}(N^2F)$	$\mathcal{O}(N^{K+1}F)$	$\mathcal{O}(N^{K+1}F + N^3)$
Expressivity	$\mathcal{O}(1)$	$\mathcal{O}(1/K)$	$\mathcal{O}(\exp^{-\sqrt{K}})$

- **Methodology:** Spatial methods traverse local regions, and generalize global patterns from the bottom-up learning, while spectral methods understand the graph from frequency perspective which leads to a top-down and global observation.
- **Computation:** Due to their methodologies, spatial methods have to conduct a number of steps on local regions to achieve convergence. Spectral methods may take one-step calculation to obtain key component for the following learning.
- **Space Complexity:** The price of spectral methods is the high space complexity, since loading the whole graph consumes a large memory storage. Spatial methods may take the whole graph when memory is efficient, and alternatively, they could employ subregion or path sampling to avoid high complexity.
- **Stability:** Spatial methods need to employ iterative algorithm to achieve the optimal, so the results may be different every time. Spectral methods rely on eigen-decomposition which is unique.

6.2 Time Complexity and Expressive Power

A-1/B-1 have a time complexity of $\mathcal{O}(N^2F)$ due to the matrix multiplication of $\mathbf{A} \mathbf{X}$. Accordingly, polynomial and rational method are analyzed in Table 5 where K is the order number. To compare their expressive power, the convergence rate on challenging jump signal is employed as a benchmark [27] (the simple signal cannot distinguish them). As shown in Table 5, A-3/B-3 converge exponentially faster than A-1/B-1, and A-2/B-2 converge linearly faster than A-1/B-1. Therefore, there is a trade-off between the expressive power and computational efficiency. A-1/B-1 have the best efficiency but only capture the linear relationship. A-3/B-3 consume the most considerable overhead but could tackle more challenging signals.

7 EXEMPLIFY THE PROPOSED FRAMEWORK

Over-smoothing and large scale issue is two of most challenging issues to existing GNNs, many recent works are proposed to tackle them with various techniques. In this section, we will show that all the improvements are still under our framework.

7.1 Sampling Point of View

To handle large graphs, the sampling mechanism is introduced as a spatial-based method. Popular methodologies include subgraph sampling and random walk.

7.1.1 Subgraph Sampling. As an early work, *GraphSAGE* [47] samples subgraph randomly, which is equivalent to employing uniform node sampling for each batch. Therefore, the transition probability follows random walk normalization ($\tilde{\mathbf{A}} = \mathbf{D}^{-1} \mathbf{A}$), making it belong to linear propagation (A-1).

Most follow-up works use the same strategy [137]: (1) build a local graph convolution for the input graph. (2) sample nodes in each layer, and (3) optimize parameters in graph convolution. Steps (2) and (3) proceed iteratively to update the weights via stochastic gradient descent [23, 24, 42, 56, 137]. To avoid the recursive neighborhood expansion, *FastGCN* [23] treats graph convolutions as integral transformation of embedding functions and proposes Monte Carlo approach to estimate the integral. Take n samples for each layer, *FastGCN* employs importance sampling to reduce variance cutting down the number of sampling nodes from product of the $n(s)$ to sum of the $n(s)$, exponentially shrinking the computational cost. *FastGCN* is proved to be importance sampling, which is better than uniform sampling, but still suffers from unstable learning when no neighbors is selected for one node and activation is zero. To avoid taxing calculation of activation, [24] further uses the historical activation in the previous layer to avoid redundant re-evaluation. [56] improves *GraphSAGE* and *FastGCN* by sampling nodes conditioned on the previous layer, and *GraphSAGE* or *FastGCN* are generalized as one variant. Learnable graph convolutional layer (LGCL) [42] selects a fixed number of neighboring nodes for each feature based on value ranking, and transform graph into 1-D data which is compatible with normal convolution networks. Similarly, [136] samples a fixed number of nodes, with different sampling policy called frontier sampling (FS). FS maintains a constant size frontier set consisting of several vertices which is randomly popped out with a degree based probability distribution. *Cluster-GCN* [28] samples a community of nodes determined by a graph clustering algorithm, and compute the graph convolution within each community.

7.1.2 Random Walk. Many variants of random walk are proposed to produce path instance, and then are feed into path learning algorithm that can derive node-level representations with word2vec [88–90]. Each path is treated as a sentence, and each node is equivalent to a word. With sufficient random walks or uniform sampling on paths, transition probability among nodes approximates to random walk normalized adjacency matrix.

As analyzed in previous section, *DeepWalk* [100] draws a number of random paths from the graph, which makes the transfer probability of random walk is, i.e., $\tilde{\mathbf{A}} = \mathbf{D}^{-1} \mathbf{A}$. Let the window size of skip-gram be $2t + 1$ and the index of current node is $t + 1$. Therefore, the updated representation is as $\mathbf{Z} = \frac{1}{t+1} \mathbf{P}(\tilde{\mathbf{A}}) \mathbf{X}$ (Eqn. 26). One popular word2vec configuration, i.e., Skip-gram with Negative Sampling (SGNS), assumes a corpus of words w and their context c . Following the work by Levy and Goldberg [70], SGNS is implicitly factorizing:

$$\log \left(\frac{|(w, c)| \cdot |\mathcal{D}|}{|w| \cdot |c|} \right) - \log b = \mathbf{A} \mathbf{B}^{\top},$$

where \mathbf{A} and \mathbf{B} denote matrix of current node and neighbors, respectively. $|(w, c)|$, $|w|$, $|c|$ and \mathcal{D} denote the number of times word-context pair (w, c) , word w , context c and corpus size, respectively;

b is the number of negative samples. Accordingly, [104] derived a exact format as:

$$\log(\mathbf{P}(\tilde{\mathbf{A}})) - \log(b) = \log\left(\frac{|E|}{T} \left(\sum_{r=1}^T (\mathbf{D}^{-1} \mathbf{A})^r\right) \mathbf{D}^{-1}\right) - \log(b),$$

where $|E|$ and T represents edge number and step size, respectively. Therefore, the target matrix to decompose is still a polynomials of \mathbf{A} .

Node2Vec [45] defines a 2nd order random walk to control the balance between Breath First Search (BFS) and Depth First Search (DFS). Assuming the random walk is sufficiently sampled, *Node2Vec*'s second order can be rewritten to decompose matrix [104]:

$$\log(\mathbf{P}(\tilde{\mathbf{A}})) - \log(b) = \log\left(\frac{\frac{1}{2T} \sum_{r=1}^T \left(\sum_u X_{w,u} \tilde{\mathbf{A}}_{c,w,u}^r + \sum_u X_{c,u} \tilde{\mathbf{A}}_{w,c,u}^r\right)}{\left(\sum_u X_{w,u}\right) \left(\sum_u X_{c,u}\right)}\right) - \log b,$$

where

$$\underline{T}_{u,v,w} = \begin{cases} \frac{1}{p} & (u,v) \in E, (v,w) \in E, u = w; \\ 1 & (u,v) \in E, (v,w) \in E, u \neq w, (w,u) \in E; \\ \frac{1}{q} & (u,v) \in E, (v,w) \in E, u \neq w, (w,u) \notin E; \\ 0 & \text{otherwise.} \end{cases}$$

$$\tilde{\mathbf{A}}_{u,v,w} = \text{Prob}(w_{j+1} = u \mid w_j = v, w_{j-1} = w) = \frac{\underline{T}_{u,v,w}}{\sum_u \underline{T}_{u,v,w}},$$

$$\mathbf{X}_{u,v} = \sum_w \tilde{\mathbf{A}}_{u,v,w} \mathbf{X}_{v,w}.$$

LINE [113] and *SDNE* [118] learn the node representations within the first- and second-order neighbors, which can be treated as unconstrained version of *Node2Vec*:

$$\log(\mathbf{P}(\tilde{\mathbf{A}})) - \log(b) = \log(|E| \tilde{\mathbf{A}}) - \log b.$$

GraphSAINT [137] employs multiple sampling polices but the best one is random walk. *PinSAGE* [133] improves the efficiency of GraphSAGE [47] by taking the top several neighbors with highest normalized visit counts.

Remark: Sampling methods, as a spatial methodology, seek both variance reduction and efficiency. With sufficient samples, subgraph and random walk are equivalent since they traverse the whole network with the transition probability associated with graph connectivity. However, no sampling method belongs to A-3 or B-3. This is reasonable since A-3/B-3 has dramatically higher computational complexity. Sampling methods significant improve the space complexity and time complexity at each step, but not necessarily reduce the total time complexity dramatically. Even though each step of computation on a subgraph sample is fast, it still requires a number of steps to achieve convergences.

7.2 Over-smoothing Point of View

We carve out two conditions under which neighborhood aggregation is not helpful: (1) when a node's neighbors are highly dissimilar and (2) when a node's embedding is already similar to that of its neighbors.

Graph neural networks have become one of the most important techniques to solve machine learning problems on graph-structured data. Recent work on vertex classification proposed deep and distributed learning models to achieve high performance and scalability. However, we find that the feature vectors of benchmark datasets are already quite informative for the classification task, and the graph structure only provides a means to denoise the data. In this paper, we develop a theoretical framework based on graph signal processing for analyzing graph neural networks. Our

results indicate that graph neural networks only perform low-pass filtering on feature vectors and do not have the non-linear manifold learning properties. We further investigate their resilience to feature noise and propose some insights on GCN-based graph neural network design.

Most GNNs perform poorly when stacking many layers, which is called the over-smoothing issue. Many related works aiming to solve the over-smoothing issue can be reduced to one category of the proposed framework [13, 22, 25, 55, 72, 73, 79, 91, 96, 108, 128, 129, 140, 143, 144]. [144] proposed a method that combines direct neighbors with higher-order, which is equivalent to polynomial propagation (A-2). Deep GCN [72, 73, 129] developed a model with a residue module, dense connection, and dilated aggregation, which learns the weights of all different orders of neighbors. This is equivalent to polynomial propagation (A-2). JKNet [128] also follows the same residue methodology as Deep GCN. DAGNN [79] stacks multiple layers which uses different orders of propagation with the learnable weights, which makes it belong to polynomial propagation (A-2). PairNorm [140] presents a two-step method that includes centering and re-scaling, which mitigates the over-smoothing from graph convolution. Therefore, PairNorm is equivalent to rational propagation (A-3), since re-scaling is similar to do propagation and restart at the same time. [13] design an adaptive method to dynamically adjust the weights between low-frequency and high-frequency components, resulting in two peaks in the spectral domain. This could also be modeled by rational propagation (A-3) with its accuracy in jump signals. DropEdge [55, 108] randomly drops a certain number of edges to avoid over-smoothing, which can be categorized as rational propagation (A-3) since dropping edge prevents the propagation and thereby provides a probability of keeping the original values of nodes. GCNII [25] applies *initial residual* which combines the smoothed representation with an initial residual connection to the first layer, and *identity mapping*, which adds an identity matrix to the weight matrix. *Initial residual* is a trick that PPAP [62] uses, which enables itself to retard the over-smoothing by keeping partial previous representations. *Identity mapping* further remains one original representation to slow down the spreading of over-smoothing propagation.

Remark: No state-of-the-art method belongs to A-1, which implies that A-1 is venerable to the over-smoothing issue. A-2 is equivalent to applying A-1 multiple times with learnable weights for different orders. Therefore, A-2 could balance low order (close to raw representations) and high orders (close to over-smoothed representations). However, too large orders of A-1 may still lead to the over-smoothing. Therefore, careful order configuration is needed for A-2. To avoid manual configuration, A-3 reserve a ratio of the final representation as raw representation regardless of the number of orders or layers.

8 OPEN PROBLEMS

Solid Theoretical Understanding Current methods are mostly heuristic approaches, which lack theoretical solutions. As GNNs make breakthroughs recently, there is a trend to understand GNNs rigorously with unified perspectives, however, with very little discussion. There is a discovery that the product of dimension of the node embeddings and the number of layers should be proportional to the scale of the graph [82]. People also found that GCNs can only learn node degrees and connected components when the number of layers grows [96]. Still, many applied math can be integrated with GNNs, such as optimal control, optimal transport, partial differential equation, differential geometry, and mean-field [11, 11, 19, 31, 60, 110].

Explainable Understanding: As a type of complex deep neural networks, GNNs can only generate prediction without any explanation, which makes them lack of self-justification. One direction is to identify its behavior is to make perturbation and identify the importance of input instance [8, 54, 68, 84, 102, 117, 134, 135]. However, the current works are still built with a black box deep

learning model, which brings more ambiguity rather than trustworthiness. Besides, most current work only generates subgraph example as an explanation, lacking a quantitative description. This emerging topic is still young, and there is no widely recognized benchmark, which is hindering progress in this direction.

Over-smoothing: As discussed, existing works that claim to be able to tackle over-smoothing incur a high computational cost. Previous works suggest that most GNNs are not deep or wide enough [82, 96]. Therefore, one way could be deepening GNNs, which might be of high complexity. Another possibility is finding adaptive filtering conditioned on the graph and attributes.

Scalability: Large scale graph is a big challenge for GNNs, and sampling is the most popular methodology, due to its reasonable trade-off between efficiency and accuracy. Another direction is to use paradigm of parallel and distributed computing [43, 64, 78].

Directed Graph: Most current work, especially spectral methods, can merely handle undirected graph due to the technique only compatible with the symmetric graph matrix. Decomposition techniques on asymmetric matrices, such as Jordan norm [59], make it possible to encode graph and filter attributes with GNN.

Dynamic Graph : Existing work model dynamic graph with GNNs and recurrent neural networks (RNNs), which remains a black box and few insights are provided. Due to the capacity of RNNs, the prediction length is limited. One possible way is to investigate network flow theory and network information theory [17, 37, 41, 71].

9 CONCLUSION

In this paper, we propose a unified framework that summarizes the state-of-the-art GNNs, providing a new perspective for understanding GNNs designed under different mechanisms. By analytically categorizing current GNNs into the spatial and spectral domains and further dividing them into subcategories, our analysis reveals that the subcategories are not only strongly connected by generalization and specialization relations within their domain, but also by equivalence relation across the domains. We demonstrate the generalization power of our proposed framework by reformulating numerous existing GNN models. The above survey of the state-of-the-art GNNs, showing that it is still a young research area. An increasing number of emerging GNN models [26, 38, 99, 120, 125, 131] make the theoretical understanding [81, 95] a urgent need. Moreover, GNNs have not been widely applied, but the interest of applying GNNs grows recently in many domains [26, 99, 120, 125, 131]. However, GNNs are still black box approaches, and researchers still want to have a better understanding of how the decisions are made by algorithms. Therefore, the next-generation GNNs are expected to be more interpretable and transparent to the target applications in various domains [8, 46, 132].

REFERENCES

- [1] Sergi Abadal, Akshay Jain, Robert Guirado, Jorge López-Alonso, and Eduard Alarcón. 2020. Computing Graph Neural Networks: A Survey from Algorithms to Accelerators. *arXiv:cs.LG/2010.00130*
- [2] Sami Abu-El-Haija, Bryan Perozzi, Amol Kapoor, Nazanin Alipourfard, Kristina Lerman, Hrayr Harutyunyan, Greg Ver Steeg, and Aram Galstyan. 2019. Mixhop: Higher-order graph convolutional architectures via sparsified neighborhood mixing. *arXiv preprint arXiv:1905.00067* (2019).
- [3] Naum I Achieser. 2013. *Theory of approximation*. Courier Corporation.
- [4] Ameya Agaskar and Yue M Lu. 2013. A Spectral Graph Uncertainty Principle. *IEEE Transactions on Information Theory* 59, 7 (2013), 4338–4356.
- [5] Lars V Ahlfors. 1953. *Complex analysis: an introduction to the theory of analytic functions of one complex variable*. New York, London (1953), 177.
- [6] Andreas Argyriou, Charles A Micchelli, and Massimiliano Pontil. 2009. When is there a representer theorem? Vector versus matrix regularizers. *Journal of Machine Learning Research* 10, Nov (2009), 2507–2529.

- [7] James Atwood and Don Towsley. 2016. Diffusion-convolutional neural networks. In *Advances in Neural Information Processing Systems*. 1993–2001.
- [8] Federico Baldassarre and Hossein Azizpour. 2019. Explainability techniques for graph convolutional networks. *arXiv preprint arXiv:1905.13686* (2019).
- [9] Michael GH Bell, Yasunori Iida, et al. 1997. Transportation network analysis. (1997).
- [10] Yoshua Bengio, Olivier Delalleau, and Nicolas Le Roux. 2006. 11 label propagation and quadratic criterion. (2006).
- [11] Martin Benning, Elena Celledoni, Matthias J Ehrhardt, Brynjulf Owren, and Carola-Bibiane Schönlieb. 2019. Deep learning as optimal control problems: Models and numerical methods. *arXiv preprint arXiv:1904.05657* (2019).
- [12] Filippo Maria Bianchi, Daniele Grattarola, Lorenzo Livi, and Cesare Alippi. 2019. Graph neural networks with convolutional arma filters. *CoRR* (2019).
- [13] Deyu Bo, Xiao Wang, Chuan Shi, and Huawei Shen. [n.d.]. Beyond Low-frequency Information in Graph Convolutional Networks. *arXiv preprint arXiv:2101.00797* ([n. d.]).
- [14] Deyu Bo, Xiao Wang, Chuan Shi, and Huawei Shen. 2021. Beyond Low-frequency Information in Graph Convolutional Networks. *Thirty-Fifth AAAI Conference on Artificial Intelligence* (2021).
- [15] Aleksandar Bojchevski, Johannes Klicpera, Bryan Perozzi, Amol Kapoor, Martin Blais, Benedek Rózemerczki, Michal Lukasik, and Stephan Günnemann. 2020. Scaling graph neural networks with approximate pagerank. In *ACM SIGKDD*. 2464–2473.
- [16] Béla Bollobás. 2004. *Extremal graph theory*. Courier Corporation.
- [17] Stephen P Borgatti. 2005. Centrality and network flow. *Social networks* 27, 1 (2005), 55–71.
- [18] John P Boyd. 2001. *Chebyshev and Fourier spectral methods*. Courier Corporation.
- [19] Pratik Prabhanjan Brahma, Dapeng Wu, and Yiyuan She. 2015. Why deep learning works: A manifold disentanglement perspective. *IEEE transactions on neural networks and learning systems* 27, 10 (2015), 1997–2008.
- [20] Michael M Bronstein, Joan Bruna, Yann LeCun, Arthur Szlam, and Pierre Vandergheynst. 2017. Geometric deep learning: going beyond euclidean data. *IEEE Signal Processing Magazine* 34, 4 (2017), 18–42.
- [21] Joan Bruna, Wojciech Zaremba, Arthur Szlam, and Yann Lecun. 2014. Spectral networks and locally connected networks on graphs. In *International Conference on Learning Representations (ICLR2014), CBLIS, April 2014*. <http://openreview.net>.
- [22] Deli Chen, Yankai Lin, Wei Li, Peng Li, Jie Zhou, and Xu Sun. 2020. Measuring and relieving the over-smoothing problem for graph neural networks from the topological view. In *Proceedings of the AAAI Conference on Artificial Intelligence*, Vol. 34. 3438–3445.
- [23] Jie Chen, Tengfei Ma, and Cao Xiao. 2018. Fastgcn: fast learning with graph convolutional networks via importance sampling. *International Conference on Learning Representations* (2018).
- [24] Jianfei Chen, Jun Zhu, and Le Song. 2018. Stochastic Training of Graph Convolutional Networks with Variance Reduction. In *International Conference on Machine Learning*. 942–950.
- [25] Ming Chen, Zhewei Wei, Zengfeng Huang, Bolin Ding, and Yaliang Li. 2020. Simple and deep graph convolutional networks. (2020).
- [26] Yu Chen, Lingfei Wu, and Mohammed J Zaki. 2019. Reinforcement learning based graph-to-sequence model for natural question generation. *arXiv preprint arXiv:1908.04942* (2019).
- [27] Z. Chen, F. Chen, R. Lai, X. Zhang, and C. Lu. 2018. Rational Neural Networks for Approximating Graph Convolution Operator on Jump Discontinuities. (2018), 59–68. <https://doi.org/10.1109/ICDM.2018.00021>
- [28] Wei-Lin Chiang, Xuanqing Liu, Si Si, Yang Li, Samy Bengio, and Cho-Jui Hsieh. 2019. Cluster-GCN: An efficient algorithm for training deep and large graph convolutional networks. In *ACM SIGKDD*.
- [29] Fan RK Chung. 1997. *Spectral graph theory*. Number 92. American Mathematical Soc.
- [30] Harold Cohen. 2011. *Numerical approximation methods*. Springer.
- [31] Nicolas Courty, Rémi Flamary, Devis Tuia, and Alain Rakotomamonjy. 2016. Optimal transport for domain adaptation. *IEEE transactions on pattern analysis and machine intelligence* 39, 9 (2016), 1853–1865.
- [32] Eric H Davidson, Jonathan P Rast, Paola Oliveri, Andrew Ransick, Cristina Calestani, Chiou-Hwa Yuh, Takuya Minokawa, Gabriele Amore, Veronica Hinman, Cesar Arenas-Mena, et al. 2002. A genomic regulatory network for development. *science* 295, 5560 (2002), 1669–1678.
- [33] Siemon de Lange, Marcel de Reus, and Martijn Van Den Heuvel. 2014. The Laplacian spectrum of neural networks. *Frontiers in computational neuroscience* 7 (2014), 189.
- [34] Siemon C de Lange, Martijn P van den Heuvel, and Marcel A de Reus. 2016. The role of symmetry in neural networks and their Laplacian spectra. *NeuroImage* 141 (2016), 357–365.
- [35] Michaël Defferrard, Xavier Bresson, and Pierre Vandergheynst. 2016. Convolutional neural networks on graphs with fast localized spectral filtering. In *Advances in neural information processing systems*. 3844–3852.
- [36] James Howard Drew and Hui Liu. 2008. Diagnosing fault patterns in telecommunication networks. US Patent 7,428,300.

- [37] Jack Edmonds and Richard M Karp. 1972. Theoretical improvements in algorithmic efficiency for network flow problems. *Journal of the ACM (JACM)* 19, 2 (1972), 248–264.
- [38] Federico Errica, Marco Podda, Davide Bacciu, and Alessio Micheli. 2019. A fair comparison of graph neural networks for graph classification. *arXiv preprint arXiv:1912.09893* (2019).
- [39] Joan Bruna Estrach, Wojciech Zaremba, Arthur Szlam, and Yann LeCun. 2014. Spectral networks and locally connected networks on graphs. In *2nd International Conference on Learning Representations, ICLR 2014*.
- [40] Gerald B Folland and Alladi Sitaram. 1997. The uncertainty principle: a mathematical survey. *Journal of Fourier analysis and applications* 3, 3 (1997), 207–238.
- [41] Lester R Ford Jr. 1956. *Network flow theory*. Technical Report. Rand Corp Santa Monica Ca.
- [42] Hongyang Gao, Zhengyang Wang, and Shuiwang Ji. 2018. Large-scale learnable graph convolutional networks. In *Proceedings of the 24th ACM SIGKDD International Conference on Knowledge Discovery & Data Mining*. 1416–1424.
- [43] Fayez Gebali. 2011. *Algorithms and parallel computing*. Wiley Online Library.
- [44] Justin Gilmer, Samuel S Schoenholz, Patrick F Riley, Oriol Vinyals, and George E Dahl. 2017. Neural message passing for quantum chemistry. In *Proceedings of the 34th International Conference on Machine Learning-Volume 70*. JMLR. org, 1263–1272.
- [45] Aditya Grover and Jure Leskovec. 2016. node2vec: Scalable feature learning for networks. In *Proceedings of the 22nd ACM SIGKDD international conference on Knowledge discovery and data mining*. ACM, 855–864.
- [46] Ruocheng Guo, Jundong Li, and Huan Liu. 2020. Learning individual treatment effects from networked observational data. *ACM International Conference on Web Search and Data Mining* (2020).
- [47] Will Hamilton, Zitao Ying, and Jure Leskovec. 2017. Inductive representation learning on large graphs. In *Advances in Neural Information Processing Systems*. 1024–1034.
- [48] William L Hamilton, Rex Ying, and Jure Leskovec. 2017. Representation learning on graphs: Methods and applications. *arXiv preprint arXiv:1709.05584* (2017).
- [49] David K Hammond, Pierre Vandergheynst, and Rémi Gribonval. 2011. Wavelets on graphs via spectral graph theory. *Applied and Computational Harmonic Analysis* 30, 2 (2011), 129–150.
- [50] Mikael Henaff, Joan Bruna, and Yann LeCun. 2015. Deep convolutional networks on graph-structured data. *arXiv preprint arXiv:1506.05163* (2015).
- [51] Mark Herbster, Massimiliano Pontil, and Lisa Wainer. 2005. Online learning over graphs. In *Proceedings of the 22nd international conference on Machine learning*. ACM, 305–312.
- [52] Geoffrey Hinton, Li Deng, Dong Yu, George Dahl, Abdel-rahman Mohamed, Navdeep Jaitly, Andrew Senior, Vincent Vanhoucke, Patrick Nguyen, Brian Kingsbury, et al. 2012. Deep neural networks for acoustic modeling in speech recognition. *IEEE Signal processing magazine* 29 (2012).
- [53] Qian Huang, Horace He, Abhay Singh, Ser-Nam Lim, and Austin R Benson. 2020. Combining Label Propagation and Simple Models Out-performs Graph Neural Networks. *arXiv preprint arXiv:2010.13993* (2020).
- [54] Qiang Huang, Makoto Yamada, Yuan Tian, Dinesh Singh, Dawei Yin, and Yi Chang. 2020. Graphlime: Local interpretable model explanations for graph neural networks. *arXiv preprint arXiv:2001.06216* (2020).
- [55] Wenbing Huang, Yu Rong, Tingyang Xu, Fuchun Sun, and Junzhou Huang. 2020. Tackling Over-Smoothing for General Graph Convolutional Networks. *arXiv:cs.LG/2008.09864*
- [56] Wenbing Huang, Tong Zhang, Yu Rong, and Junzhou Huang. 2018. Adaptive sampling towards fast graph representation learning. *Advances in neural information processing systems* 31 (2018), 4558–4567.
- [57] E. Isufi, A. Loukas, A. Simonetto, and G. Leus. 2017. Autoregressive Moving Average Graph Filtering. *IEEE Transactions on Signal Processing* 65, 2 (Jan 2017), 274–288. <https://doi.org/10.1109/TSP.2016.2614793>
- [58] Rie Johnson and Tong Zhang. 2007. On the effectiveness of Laplacian normalization for graph semi-supervised learning. *Journal of Machine Learning Research* 8, Jul (2007), 1489–1517.
- [59] Bo Kågström and Axel Ruhe. 1980. An algorithm for numerical computation of the Jordan normal form of a complex matrix. *ACM Transactions on Mathematical Software (TOMS)* 6, 3 (1980), 398–419.
- [60] Tatsuro Kawamoto, Masashi Tsubaki, and Tomoyuki Obuchi. 2019. Mean-field theory of graph neural networks in graph partitioning. *Journal of Statistical Mechanics: Theory and Experiment* 2019, 12 (2019), 124007.
- [61] Thomas N Kipf and Max Welling. 2017. Semi-supervised classification with graph convolutional networks. *ICLR* (2017).
- [62] Johannes Klicpera, Aleksandar Bojchevski, and Stephan Günnemann. 2018. Predict then propagate: Graph neural networks meet personalized pagerank. (2018).
- [63] Johannes Klicpera, Stefan Weißberger, and Stephan Günnemann. 2019. Diffusion improves graph learning. In *Advances in Neural Information Processing Systems*. 13354–13366.
- [64] Ajay D Kshemkalyani and Mukesh Singhal. 2011. *Distributed computing: principles, algorithms, and systems*. Cambridge University Press.

- [65] David Lazer, Alex Sandy Pentland, Lada Adamic, Sinan Aral, Albert Laszlo Barabasi, Devon Brewer, Nicholas Christakis, Noshir Contractor, James Fowler, Myron Gutmann, et al. 2009. Life in the network: the coming age of computational social science. *Science (New York, NY)* 323, 5915 (2009), 721.
- [66] Yann LeCun, Yoshua Bengio, and Geoffrey Hinton. 2015. Deep learning. *nature* 521, 7553 (2015), 436.
- [67] John Boaz Lee, Ryan A. Rossi, Sungchul Kim, Nesreen K. Ahmed, and Eunye Koh. 2019. Attention Models in Graphs: A Survey. *ACM Trans. Knowl. Discov. Data* 13, 6, Article Article 62 (Nov. 2019), 25 pages. <https://doi.org/10.1145/3363574>
- [68] Jure Leskovec. 2019. GNNExplainer: Generating Explanations for Graph Neural Networks. (2019).
- [69] Ron Levie, Federico Monti, Xavier Bresson, and Michael M Bronstein. 2018. Cayleynets: Graph convolutional neural networks with complex rational spectral filters. *IEEE Transactions on Signal Processing* 67, 1 (2018), 97–109.
- [70] Omer Levy and Yoav Goldberg. 2014. Neural word embedding as implicit matrix factorization. *Advances in neural information processing systems* 27 (2014), 2177–2185.
- [71] Bingdong Li, Jeff Springer, George Bebis, and Mehmet Hadi Gunes. 2013. A survey of network flow applications. *Journal of Network and Computer Applications* 36, 2 (2013), 567–581.
- [72] Guohao Li, Matthias Muller, Ali Thabet, and Bernard Ghanem. 2019. Deepgcns: Can gcns go as deep as cnns?. In *Proceedings of the IEEE/CVF International Conference on Computer Vision*. 9267–9276.
- [73] Guohao Li, Chenxin Xiong, Ali Thabet, and Bernard Ghanem. 2020. Deepergcn: All you need to train deeper gcns. *arXiv preprint arXiv:2006.07739* (2020).
- [74] Qimai Li, Zhichao Han, and Xiao-Ming Wu. 2018. Deeper insights into graph convolutional networks for semi-supervised learning. In *Thirty-Second AAAI Conference on Artificial Intelligence*.
- [75] Qimai Li, Xiao-Ming Wu, Han Liu, Xiaotong Zhang, and Zhichao Guan. 2019. Label Efficient Semi-Supervised Learning via Graph Filtering. In *The IEEE Conference on Computer Vision and Pattern Recognition (CVPR)*.
- [76] Xiaomin Liang, Daifeng Li, and Andrew Madden. 2020. Attributed Network Embedding based on Mutual Information Estimation. In *Proceedings of the 29th ACM International Conference on Information & Knowledge Management*. 835–844.
- [77] Yankai Lin, Zhiyuan Liu, Maosong Sun, Yang Liu, and Xuan Zhu. 2015. Learning entity and relation embeddings for knowledge graph completion.. In *AAAI*, Vol. 15. 2181–2187.
- [78] Husong Liu, Shengliang Lu, Xinyu Chen, and Bingsheng He. 2020. G3: when graph neural networks meet parallel graph processing systems on GPUs. *Proceedings of the VLDB Endowment* 13, 12 (2020), 2813–2816.
- [79] Meng Liu, Hongyang Gao, and Shuiwang Ji. 2020. Towards deeper graph neural networks. In *Proceedings of the 26th ACM SIGKDD International Conference on Knowledge Discovery & Data Mining*. 338–348.
- [80] Xin Liu, Tsuyoshi Murata, Kyoung-Sook Kim, Chatchawan Kotarasu, and Chenyi Zhuang. 2019. A general view for network embedding as matrix factorization. In *Proceedings of the Twelfth ACM International Conference on Web Search and Data Mining*. 375–383.
- [81] Andreas Loukas. 2019. What graph neural networks cannot learn: depth vs width. *arXiv preprint arXiv:1907.03199* (2019).
- [82] Andreas Loukas. 2020. What graph neural networks cannot learn: depth vs width. In *International Conference on Learning Representations*. <https://openreview.net/forum?id=B1l2bp4YwS>
- [83] A. Loukas, A. Simonetto, and G. Leus. 2015. Distributed Autoregressive Moving Average Graph Filters. *IEEE Signal Processing Letters* 22, 11 (Nov 2015), 1931–1935. <https://doi.org/10.1109/LSP.2015.2448655>
- [84] Dongsheng Luo, Wei Cheng, Dongkuan Xu, Wenchao Yu, Bo Zong, Haifeng Chen, and Xiang Zhang. 2020. Parameterized explainer for graph neural network. *arXiv preprint arXiv:2011.04573* (2020).
- [85] Thang Luong, Hieu Pham, and Christopher D Manning. 2015. Effective Approaches to Attention-based Neural Machine Translation. In *Proceedings of the 2015 Conference on Empirical Methods in Natural Language Processing*. 1412–1421.
- [86] Vivien Marx. 2012. High-throughput anatomy: charting the brain’s networks. *Nature* 490, 7419 (2012), 293.
- [87] John C Mason and David C Handscomb. 2002. *Chebyshev polynomials*. CRC Press.
- [88] Tomas Mikolov, Kai Chen, Greg Corrado, and Jeffrey Dean. 2013. Efficient estimation of word representations in vector space. *Workshop at ICLR* (2013).
- [89] Tomas Mikolov, Ilya Sutskever, Kai Chen, Greg S Corrado, and Jeff Dean. 2013. Distributed representations of words and phrases and their compositionality. *Advances in neural information processing systems* 26 (2013), 3111–3119.
- [90] Tomáš Mikolov, Wen-tau Yih, and Geoffrey Zweig. 2013. Linguistic regularities in continuous space word representations. In *NAACL*. 746–751.
- [91] Yimeng Min, Frederik Wenkel, and Guy Wolf. 2020. Scattering gcn: Overcoming oversmoothness in graph convolutional networks. *arXiv preprint arXiv:2003.08414* (2020).
- [92] Federico Monti, Davide Boscaini, Jonathan Masci, Emanuele Rodola, Jan Svoboda, and Michael M Bronstein. 2017. Geometric deep learning on graphs and manifolds using mixture model cnns. In *Proceedings of the IEEE Conference on Computer Vision and Pattern Recognition*. 5115–5124.
- [93] Mark EJ Newman. 2002. Spread of epidemic disease on networks. *Physical review E* 66, 1 (2002), 016128.

- [94] Hoang NT and Takanori Maehara. 2019. Revisiting graph neural networks: All we have is low-pass filters. *arXiv preprint arXiv:1905.09550* (2019).
- [95] Kenta Oono and Taiji Suzuki. [n.d.]. GRAPH NEURAL NETWORKS EXPONENTIALLY LOSE EXPRESSIVE POWER FOR NODE CLASSIFICATION. ([n. d.]).
- [96] Kenta Oono and Taiji Suzuki. 2019. Graph Neural Networks Exponentially Lose Expressive Power for Node Classification. In *International Conference on Learning Representations*.
- [97] Alan V Oppenheim, John R Buck, and Ronald W Schafer. 2001. *Discrete-time signal processing*. Vol. 2. Upper Saddle River, NJ: Prentice Hall.
- [98] Ricardo Pachon. 2010. *Algorithms for polynomial and rational approximation*. Ph.D. Dissertation. University of Oxford.
- [99] Cheol Woo Park and Chris Wolverton. 2019. Developing an improved Crystal Graph Convolutional Neural Network framework for accelerated materials discovery. *arXiv:physics.comp-ph/1906.05267*
- [100] Bryan Perozzi, Rami Al-Rfou, and Steven Skiena. 2014. Deepwalk: Online learning of social representations. In *Proceedings of the 20th ACM SIGKDD international conference on Knowledge discovery and data mining*. ACM, 701–710.
- [101] Penco Petrov Petrushev and Vasil Atanasov Popov. 2011. *Rational approximation of real functions*. Vol. 28. Cambridge University Press.
- [102] Phillip E Pope, Soheil Kolouri, Mohammad Rostami, Charles E Martin, and Heiko Hoffmann. 2019. Explainability methods for graph convolutional neural networks. In *Proceedings of the IEEE/CVF Conference on Computer Vision and Pattern Recognition*. 10772–10781.
- [103] Michael James David Powell. 1981. *Approximation theory and methods*. Cambridge university press.
- [104] Jiezhong Qiu, Yuxiao Dong, Hao Ma, Jian Li, Kuansan Wang, and Jie Tang. 2018. Network embedding as matrix factorization: Unifying deepwalk, line, pte, and node2vec. In *Proceedings of the Eleventh ACM International Conference on Web Search and Data Mining*. 459–467.
- [105] Joseph Redmon, Santosh Divvala, Ross Girshick, and Ali Farhadi. 2016. You only look once: Unified, real-time object detection. In *Proceedings of the IEEE conference on computer vision and pattern recognition*. 779–788.
- [106] Eugene Y Remez. 1934. Sur la détermination des polynômes d’approximation de degré donnée. *Comm. Soc. Math. Kharkov* 10 (1934), 41–63.
- [107] Shaoqing Ren, Kaiming He, Ross Girshick, and Jian Sun. 2015. Faster r-cnn: Towards real-time object detection with region proposal networks. In *Advances in neural information processing systems*. 91–99.
- [108] Yu Rong, Wenbing Huang, Tingyang Xu, and Junzhou Huang. 2019. Dropedge: Towards deep graph convolutional networks on node classification. In *International Conference on Learning Representations*.
- [109] Emanuele Rossi, Fabrizio Frasca, Ben Chamberlain, Davide Eynard, Michael Bronstein, and Federico Monti. 2020. SIGN: Scalable Inception Graph Neural Networks. *arXiv preprint arXiv:2004.11198* (2020).
- [110] Lars Ruthotto and Eldad Haber. 2019. Deep neural networks motivated by partial differential equations. *Journal of Mathematical Imaging and Vision* (2019), 1–13.
- [111] B Schölkopf, R Herbrich, and AJ Smola. 2001. A generalized representer theorem Computational Learning Theory ed D Helmbold and B Williamson.
- [112] David I Shuman, Sunil K Narang, Pascal Frossard, Antonio Ortega, and Pierre Vandergheynst. 2013. The emerging field of signal processing on graphs: Extending high-dimensional data analysis to networks and other irregular domains. *IEEE Signal Processing Magazine* 30, 3 (2013), 83–98.
- [113] Jian Tang, Meng Qu, Mingzhe Wang, Ming Zhang, Jun Yan, and Qiaozhu Mei. 2015. Line: Large-scale information network embedding. In *Proceedings of the 24th international conference on world wide web*.
- [114] Lloyd N Trefethen. 2013. *Approximation theory and approximation practice*. Vol. 128. Siam.
- [115] Petar Veličković, Guillem Cucurull, Arantxa Casanova, Adriana Romero, Pietro Liò, and Yoshua Bengio. 2018. Graph Attention Networks. (2018).
- [116] Petar Veličković, William Fedus, William L Hamilton, Pietro Liò, Yoshua Bengio, and R Devon Hjelm. 2018. Deep Graph Infomax. In *International Conference on Learning Representations*.
- [117] Minh N Vu and My T Thai. 2020. Pgm-explainer: Probabilistic graphical model explanations for graph neural networks. *arXiv preprint arXiv:2010.05788* (2020).
- [118] Daixin Wang, Peng Cui, and Wenwu Zhu. 2016. Structural deep network embedding. In *Proceedings of the 22nd ACM SIGKDD international conference on Knowledge discovery and data mining*. 1225–1234.
- [119] Yewen Wang, Ziniu Hu, Yusong Ye, and Yizhou Sun. 2020. Demystifying Graph Neural Network Via Graph Filter Assessment. <https://openreview.net/forum?id=r1erNxBtwr>
- [120] Mark Weber, Giacomo Domeniconi, Jie Chen, Daniel Karl I Weidele, Claudio Bellei, Tom Robinson, and Charles E Leiserson. 2019. Anti-money laundering in bitcoin: Experimenting with graph convolutional networks for financial forensics. *arXiv preprint arXiv:1908.02591* (2019).
- [121] Felix Wu, Amauri Souza, Tianyi Zhang, Christopher Fifty, Tao Yu, and Kilian Weinberger. 2019. Simplifying Graph Convolutional Networks. In *International Conference on Machine Learning*. 6861–6871.

- [122] Xiao-Ming Wu, Zhenguo Li, Anthony M So, John Wright, and Shih-Fu Chang. 2012. Learning with partially absorbing random walks. In *Advances in neural information processing systems*. 3077–3085.
- [123] Yonghui Wu, Mike Schuster, Zhifeng Chen, Quoc V Le, Mohammad Norouzi, Wolfgang Macherey, Maxim Krikun, Yuan Cao, Qin Gao, Klaus Macherey, et al. 2016. Google’s neural machine translation system: Bridging the gap between human and machine translation. *arXiv preprint arXiv:1609.08144* (2016).
- [124] Zonghan Wu, Shirui Pan, Fengwen Chen, Guodong Long, Chengqi Zhang, and Philip S Yu. 2019. A comprehensive survey on graph neural networks. *arXiv preprint arXiv:1901.00596* (2019).
- [125] Tian Xie and Jeffrey C. Grossman. 2018. Crystal Graph Convolutional Neural Networks for an Accurate and Interpretable Prediction of Material Properties. *Phys. Rev. Lett.* 120 (Apr 2018), 145301. Issue 14.
- [126] Keyulu Xu, Weihua Hu, Jure Leskovec, and Stefanie Jegelka. 2018. How powerful are graph neural networks? *arXiv preprint arXiv:1810.00826* (2018).
- [127] Keyulu Xu, Weihua Hu, Jure Leskovec, and Stefanie Jegelka. 2019. How Powerful are Graph Neural Networks?. In *International Conference on Learning Representations*. <https://openreview.net/forum?id=ryGs6iA5Km>
- [128] Keyulu Xu, Chengtao Li, Yonglong Tian, Tomohiro Sonobe, Ken-ichi Kawarabayashi, and Stefanie Jegelka. 2018. Representation learning on graphs with jumping knowledge networks. *arXiv preprint arXiv:1806.03536* (2018).
- [129] Chaoqi Yang, Ruijie Wang, Shuochao Yao, Shengzhong Liu, and Tarek Abdelzaher. 2020. Revisiting" over-smoothing" in deep gcns. *arXiv preprint arXiv:2003.13663* (2020).
- [130] Carl Yang, Yuxin Xiao, Yu Zhang, Yizhou Sun, and Jiawei Han. 2020. Heterogeneous Network Representation Learning: Survey, Benchmark, Evaluation, and Beyond. *arXiv preprint arXiv:2004.00216* (2020).
- [131] Fan Yang, Zhilin Yang, and William W Cohen. 2017. Differentiable learning of logical rules for knowledge base reasoning. In *Advances in Neural Information Processing Systems*. 2319–2328.
- [132] Rex Ying, Dylan Bourgeois, Jiaxuan You, Marinka Zitnik, and Jure Leskovec. 2019. GNN Explainer: A Tool for Post-hoc Explanation of Graph Neural Networks. (2019).
- [133] Rex Ying, Ruining He, Kaifeng Chen, Pong Eksombatchai, William L Hamilton, and Jure Leskovec. 2018. Graph convolutional neural networks for web-scale recommender systems. In *ACM SIGKDD*. 974–983.
- [134] Hao Yuan, Jiliang Tang, Xia Hu, and Shuiwang Ji. 2020. Xgmn: Towards model-level explanations of graph neural networks. In *ACM SIGKDD*. 430–438.
- [135] Hao Yuan, Haiyang Yu, Shurui Gui, and Shuiwang Ji. 2020. Explainability in Graph Neural Networks: A Taxonomic Survey. *arXiv preprint arXiv:2012.15445* (2020).
- [136] Hanqing Zeng, Hongkuan Zhou, Ajitesh Srivastava, Rajgopal Kannan, and Viktor Prasanna. 2019. Accurate, efficient and scalable graph embedding. In *2019 IEEE International Parallel and Distributed Processing Symposium (IPDPS)*. IEEE, 462–471.
- [137] Hanqing Zeng, Hongkuan Zhou, Ajitesh Srivastava, Rajgopal Kannan, and Viktor Prasanna. 2019. Graphsaint: Graph sampling based inductive learning method. *International Conference on Learning Representations* (2019).
- [138] Songyang Zhang, Xuming He, and Shipeng Yan. 2019. Latentgmn: Learning efficient non-local relations for visual recognition. In *International Conference on Machine Learning*. PMLR, 7374–7383.
- [139] Ziwei Zhang, Peng Cui, and Wenwu Zhu. 2018. Deep learning on graphs: A survey. *arXiv preprint arXiv:1812.04202* (2018).
- [140] Lingxiao Zhao and Leman Akoglu. 2019. PairNorm: Tackling Oversmoothing in GNNs. In *International Conference on Learning Representations*.
- [141] Dengyong Zhou, Olivier Bousquet, Thomas N Lal, Jason Weston, and Bernhard Schölkopf. 2004. Learning with local and global consistency. In *Advances in neural information processing systems*. 321–328.
- [142] Jie Zhou, Ganqu Cui, Zhengyan Zhang, Cheng Yang, Zhiyuan Liu, and Maosong Sun. 2018. Graph neural networks: A review of methods and applications. *arXiv preprint arXiv:1812.08434* (2018).
- [143] Kaixiong Zhou, Xiao Huang, Yuening Li, Daochen Zha, Rui Chen, and Xia Hu. 2020. Towards Deeper Graph Neural Networks with Differentiable Group Normalization. *arXiv:cs.LG/2006.06972*
- [144] Jiong Zhu, Yujun Yan, Lingxiao Zhao, Mark Heimann, Leman Akoglu, and Danai Koutra. 2020. Beyond Homophily in Graph Neural Networks: Current Limitations and Effective Designs. *NeurIPS* (2020).
- [145] Meiqi Zhu, Xiao Wang, Chuan Shi, Houye Ji, and Peng Cui. 2021. Interpreting and Unifying Graph Neural Networks with An Optimization Framework. *arXiv preprint arXiv:2101.11859* (2021).
- [146] Xiaojin Zhu, Zoubin Ghahramani, and John D Lafferty. 2003. Semi-supervised learning using gaussian fields and harmonic functions. In *Proceedings of the 20th International conference on Machine learning (ICML-03)*. 912–919.
- [147] Xiaofan Zhu and Michael Rabbat. 2012. Approximating signals supported on graphs. In *Acoustics, Speech and Signal Processing (ICASSP), 2012 IEEE International Conference on*. IEEE, 3921–3924.
- [148] Chenyi Zhuang and Qiang Ma. 2018. Dual graph convolutional networks for graph-based semi-supervised classification. In *Proceedings of the 2018 World Wide Web Conference*. 499–508.
- [149] Eric Ziegel. 1987. Numerical recipes: the art of scientific computing.